MOLECULAR AND CELLULAR BIOLOGY, Jan. 2005, p. 575–589 Vol. 25, No. 2
0270-7306/05/$08.00+0 doi:10.1128/MCB.25.2.575–589.2005

Phosphatidylinositol 3-Kinase-Mediated Effects of Glucose on Vacuolar H^+-ATPase Assembly, Translocation, and Acidification of Intracellular Compartments in Renal Epithelial Cells†

Yuri Y. Sautin,[1]* Ming Lu,[2] Andrew Gaugler,[1] Li Zhang,[1] and Stephen L. Gluck[2]

Department of Medicine, University of Florida College of Medicine, Gainesville, Florida,[1] and Department of Medicine, University of California, San Francisco, San Francisco, California[2]

Received 22 March 2004/Returned for modification 25 June 2004/Accepted 20 October 2004

Vacuolar H^+-ATPases (V-ATPases) are a family of ATP-driven proton pumps. They maintain pH gradients between intracellular compartments and are required for proton secretion out of the cytoplasm. Mechanisms of extrinsic control of V-ATPase are poorly understood. Previous studies showed that glucose is an important regulator of V-ATPase assembly in *Saccharomyces cerevisiae*. Human V-ATPase directly interacts with aldolase, providing a coupling mechanism for glucose metabolism and V-ATPase function. Here we show that glucose is a crucial regulator of V-ATPase in renal epithelial cells and that the effect of glucose is mediated by phosphatidylinositol 3-kinase (PI3K). Glucose stimulates V-ATPase-dependent acidification of the intracellular compartments in human proximal tubular cells HK-2 and porcine renal epithelial cells LLC-PK_1. Glucose induces rapid ATP-independent assembly of the V_1 and V_o domains of V-ATPase and extensive translocation of the V-ATPase V_1 and V_o domains between different membrane pools and between membranes and the cytoplasm. In HK-2 cells, glucose stimulates polarized translocation of V-ATPase to the apical plasma membrane. The effects of glucose on V-ATPase trafficking and assembly can be abolished by pretreatment with the PI3K inhibitor LY294002 and can be reproduced in glucose-deprived cells by adenoviral expression of the constitutively active catalytic subunit p110α of PI3K. Taken together these data provide evidence that, in renal epithelial cells, glucose plays an important role in the control of V-ATPase-dependent acidification of intracellular compartments and V-ATPase assembly and trafficking and that the effects of glucose are mediated by PI3K-dependent signaling.

Vacuolar H^+-ATPases (V-ATPases) are a family of electrogenic ATP-driven proton pumps which function in almost every eukaryotic cell. V-ATPases are required to maintain proton gradients between intracellular compartments and for proton secretion from the plasma membrane of certain specialized cells (reviewed in references 32, 42, and 43). In the intracellular compartments, V-ATPases acidify early and late endosomes, lysosomes, and Golgi-derived secretory vesicles, providing the motive force and optimal pH for internalization and dissociation of ligand-receptor complexes, pH-driven secretion, and activation of lysosomal enzymes for protein processing and degradation (43, 48). Plasma membrane V-ATPases are essential for acid secretion and bicarbonate transport in the proximal tubule and collecting duct of the kidney, pH homeostasis in macrophages and neutrophils, acidification of the extracellular environment by certain tumor cells, and K^+ secretion in insect midgut cells, (24, 43). V-ATPase-dependent acidification of the extracellular compartment between the osteoclast ruffled membrane and the bone surface is crucial for bone remodeling (23).

V-ATPase is a large, multisubunit protein. It is composed of at least 13 subunits with a total molecular mass of about 900 kDa and has two domains, the V_1 domain (catalytic, membrane-associated, 640 kDa) and V_o domain (membrane spanning, 260 kDa). The V_1 domain is responsible primarily for ATP hydrolysis. It consists of eight different subunits (A to H) in a stoichiometry of $A_3B_3CDEFG_2H_{1-2}$. V_1 attaches to the proton-translocating V_o domain, which is composed of five subunits (a, b, c, c′, and c″) in a stoichiometry of abc′c″c_4 (20, 32, 43).

Regulation of V-ATPase function in response to physiological stimuli is thought to be a multilevel process. It includes control of the expression of V-ATPase subunit genes (34, 62), intracellular targeting and translocation from vesicles to the plasma membrane (2, 9, 10), and reversible dissociation of the V_o and V_1 domains, entailing inactivation of the pump (30, 31, 55).

Several extrinsic regulatory factors have been reported to control V-ATPase-mediated proton transport. They include bicarbonate concentration and the closely related parameters pH and pCO_2, mineralocorticoid hormones, endothelin, angiotensin II (reviewed in references 23 and 24), and cytokines, such as interleukin-1 (IL-1) (7) and IL-4 and -13 (59). The underlying intracellular signaling mechanisms remain largely unknown. Involvement of G proteins and protein kinases A and C has been implicated in several studies (23, 24). The E subunit of V-ATPase is able to interact directly with the Dbl homology domain of the guanine nucleotide exchange factor

* Corresponding author. Mailing address: Department of Medicine, Division of Nephrology, Box 100224, University of Florida, 1600 SW Archer Rd., Gainesville, FL 32610-0224. Phone: (352) 392-2448. Fax: (352) 392-5465. E-mail: sautiyy@medicine.ufl.edu.

† Supplemental material for this article may be found at http://mcb.asm.org/.

mSOS, linking V-ATPase with the small G protein Rac1 (39). A recent study demonstrated the role of bicarbonate-activated soluble adenylyl cyclase and cyclic AMP-dependent signal transduction in pH-dependent V-ATPase recycling (45).

Among the most intriguing functions of V-ATPase is its ability to respond to extracellular glucose. In the yeast *Saccharomyces cerevisiae*, glucose deprivation produced rapid and reversible dissociation of the V-ATPase into V_1 and V_o domains (30). In *S. cerevisiae*, this mechanism regulates the balance between the conservation of cytoplasmic ATP and maintenance of intracellular pH homeostasis (31). In human kidney, subunit E of V-ATPase interacts directly with the glycolytic enzyme aldolase (35, 36) and subunit a interacts with phosphofructokinase-1 (54), thereby providing a coupling mechanism with the glycolytic pathway. The kidney has the most V-ATPase activity among mammalian tissues, and within the kidney, V-ATPase is most abundant in epithelial cells of the initial segments of the proximal tubule and in intercalated cells of the collecting duct (24). Therefore, in kidney epithelia, the response of V-ATPase to glucose may represent a pivotal regulatory mechanism.

The mechanism by which glucose regulates V-ATPase remains unclear. In *S. cerevisiae*, V-ATPase assembly in response to glucose did not involve the Ras-cyclic AMP pathway, Snf1p (the homolog of the mammalian fuel sensor protein kinase AMPK), protein kinase C, or the general stress response protein Rts1p (homolog of the mammalian B-regulatory subunit of protein phosphatase A_2) (44). These results showed that the reversible disassembly of the V-ATPase in *S. cerevisiae* does not require any known glucose-induced signaling pathway (31) On the other hand, V-ATPase assembly depends on the Skp1-containing adaptor complex RAVE, suggesting involvement of intracellular signaling (49, 51). Furthermore, glucose-induced activation of plasma membrane V-ATPase in *S. cerevisiae* is likely to be activated via phosphatidylinositol-type signaling involving protein kinase C (6). In the ruffled border of osteoclasts, V-ATPase is localized along with phosphatidylinositol 3-kinase (PI3K) (40). Wortmannin, a specific inhibitor of PI3K, inhibited the formation of ruffled border and osteoclastic bone resorption (40, 41), suggesting involvement of PI3K-dependent signaling in the control of V-ATPase. However, the biochemical mechanism of the glucose effects on V-ATPase in mammalian cells remains unknown.

In the present study, we demonstrated that glucose is a potent regulator of V-ATPase in kidney proximal tubular cells in vitro. We showed that glucose stimulates acidification of intracellular compartments by V-ATPase and that this effect is mediated by PI3K. Glucose removal diminished V-ATPase-dependent acidification, decreased ATP hydrolytic activity of V-ATPase, induced its disassembly into V_o and V_1 domains, and led to translocation of both V_1 and V_o from plasma membrane and submembrane vesicles to intracellular vesicles (V_1 and V_o) and the cytoplasm (V_1). Glucose stimulation induces V-ATPase activity, reassembly, and translocation to the vesicular and plasma membranes and fast acidification of intracellular compartments. Glucose flux through the glycolytic pathway is not required to provide a signal for V-ATPase assembly. Active PI3K is required for the glucose-induced changes in V-ATPase assembly and trafficking. Adenoviral expression of the constitutively active p110α catalytic subunit of PI3K mimics the effect of glucose in cells maintained in glucose-free conditions. These results suggest that, in renal epithelial cells, glucose is a physiological regulator of acidification of intracellular compartments and V-ATPase activity, assembly, and trafficking and that its effects are mediated by the PI3K signaling pathway.

MATERIALS AND METHODS

Cell culture. Porcine kidney proximal tubule-like cell line LLC-PK_1 (46) and the human proximal tubule cell line HK-2 (47) were used. Prior to experiments, LLC-PK_1 cells were maintained in 199 medium (Life Technologies, Rockville, Md.) containing 10% fetal bovine serum (FBS), 100 U of penicillin/ml, and 100 μg of streptomycin/ml. HK-2 cells were maintained in Dulbecco's modified Eagle's medium (DMEM)–F-12 medium (1:1) (Life Technologies) supplemented with 10% fetal calf serum, insulin (10 mg/liter), transferrin (5.5 mg/liter), sodium selenite (6.7 μg/liter), and antibiotics. Seventy to eighty percent confluent cultures were used for experiments. Packaging HEK 293 cells were maintained in DMEM medium supplemented with 10% FBS, 100 U of penicillin/ml, and 100 μg of streptomycin/ml.

Recombinant adenoviral vector for constitutively active p110α catalytic subunit of PI3K. To construct an adenoviral vector for constitutively active PI3K, we used the Adeno-X expression system (Clontech Laboratories Inc., Palo Alto, Calif.). cDNA for Myc-tagged constitutively active PI3K (coding sequence for bovine p110α fused with the amino-terminal myristoylation signal site from the *src*-p60 oncogene and carboxy-terminal Myc tag: Myr-p110-Myc) in a pBluescript plasmid was obtained from W. Ogawa (Kobe University School of Medicine, Kobe, Japan) (33). Myr-p110-Myc was amplified from the vector by PCR with primers containing restriction sites for NheI and AflII. It was cloned into the pShuttle vector, using NheI/AflII restriction sites in the multiple cloning site region. Kanamycin-resistant transformants were selected following transformation of DH5α. The expression cassette containing Myr-p110-Myc was excised from recombinant pShuttle by double digestion with I-CeuI/PI-SceI and ligated into the Adeno-X vector linearized with I-CeuI/PI-SceI. The ligation product was digested with SwaI to remove nonrecombinant Adeno-X vector background followed by transformation of DH5α. Ampicillin-resistant transformants were selected, and recombinant adenoviral DNA was isolated and analyzed by combining the following approaches: (i) PCR with Adeno-X PCR Primer Set 2 (Clontech Laboratories), amplifying a 312-bp segment of pAdeno-X viral DNA only from recombinant DNA that contained expression cassette inserts derived from pShuttle; (ii) double digestion of the recombinant adenoviral DNA with I-CeuI/PI-SceI, which produced a fragment of the expected size (4.5 kb); and (iii) verification of the construct by ABI Prism BigDye Terminator cycle sequencing (Applied Biosystems).

Recombinant adenoviral DNA was linearized with PacI. HEK 293 packaging cells were transfected with a linearized vector, using Lipofectamine 2000 (Life Technologies). Packaged replication-defective adenovirus was amplified, isolated, and titrated according to the protocol of the manufacturer of the Adeno-X expression system. Expression of the constitutively active p110 catalytic subunit of PI3K after infection of packaging and target cells with recombinant adenovirus, named Adeno/Myr-p110-Myc, at a multiplicity of infection (MOI) of 10 to 25 was confirmed by (i) detection of Myc-tagged protein of the expected molecular mass (110 kDa) 24 to 48 h postinfection, using immunoblotting of cell extracts with Myc-tag (9B11) monoclonal antibody (Cell Signaling Technology, Beverly, Mass.) (see Fig. S1a in the supplemental material) and (ii) demonstration that overexpression of Myr-p110-Myc delivered with Adeno/Myr-p110-Myc is sufficient to substitute serum in maintaining a high level of the activated (phosphorylated) downstream protein kinase Akt in serum-deprived HK-2 (see Fig. S1b in the supplemental material). Preliminary experiments showed that serum-induced phosphorylation of Akt in Hk-2 and LLC-PK_1 cells is mediated by PI3K (data not shown). Similarly, we constructed recombinant *lacZ*-containing adenovirus by using the pShuttle-lacZ vector (Clontech Laboratories). Expression of β-galactosidase (β-Gal) was detected by using the β-Gal staining kit (Invitrogen, Carlsbad, Calif.). In all experiments with adenoviral infection, Adeno-LacZ was used as a control and cells were infected at an MOI of 10 for both adenoviruses, providing 80 to 90% infection rates at 48 h postinfection, as shown by preliminary experiments.

V-ATPase antibodies. Anti-V-ATPase monoclonal antibody (MAb) H6.1 (21, 64), E-subunit-specific MAb E11 (27), and B1-specific polyclonal antibody (34) were previously characterized. To generate isoform nonspecific antibody for subunit a ("pan-a"), the conserved sequence FRSEEMCLSQLFLQ in the N-terminal domain of the human a4 subunit was chosen. Rabbit polyclonal anti-

bodies to this keyhole limpet hemocyanin-conjugated peptide were generated by Research Genetics (InVitrogen Corporation, Carlsbad, Calif.). The antibody was purified from the antiserum on an immobilized protein A column, using the ImmunoPure Plus(A) immunoglobulin G (IgG) purification kit (Pierce, Rockford Ill.) or on an affinity column with FRSEEMCLSQLFLQ peptide immobilized on cross-linked beaded agarose, using the AminoLink kit from Pierce. The FRSEEMCLSQLFLQ peptide was synthesized, purified by high-performance liquid chromatography, and analyzed by mass spectrometry (Sigma/Genosys, The Woodlands, Tex.). This antibody recognizes protein with an M_r of ≈110, and specificity of immunoreactivity was confirmed by peptide competition analysis with FRSEEMCLSQLFLQ (see Fig. S2 in the supplemental material).

Immunoprecipitation and assays of V-ATPase assembly and activity. LLC-PK_1 cells were cultured to 75 to 80% confluence. Then they were incubated overnight in glucose-free DMEM (Life Technologies) with or without dialyzed FBS containing a residual concentration of glucose. Then the cells were stimulated with 10 mM glucose and/or 20 mM 2-deoxyglucose for 15 min. For PI3K inhibition the cells were preincubated with 25 μM LY294002 30 min prior to addition of glucose. Immunoprecipitation of V-ATPase was performed using H6.1, an E-subunit (V_1)-specific MAb (21). Cells were washed with ice-cold phosphate-buffered saline (PBS) and lysed with buffer containing 20 mM Tris-HCl (pH 7.3), 1.5% nonylglucoside, 0.6% 3-[(3-cholamidopropyl)dimethylammonio]-1-propanesulfonate (CHAPS), 1 mM dithiothreitol, 1 mM EDTA, 1 mM EGTA, 10% glycerol, 2 mM sodium orthovanadate, 1 mM phenylmethylsulfonyl fluoride, 40 μg of leupeptin/ml, 5 μg of aprotinin/ml, and 1 μg of pepstatin/ml. Determination of protein in the supernatant (protein extract) was performed using the bicinchoninic acid (BCA) protein assay (Pierce). Following centrifugation (10 min at 12,000 × *g*, 4°C) to remove insoluble material, the cell extracts were incubated with protein A-agarose beads (Pierce) to eliminate proteins nonspecifically bound to protein A. To prepare the immunobead complex, 30 μl of protein A-agarose was washed with 20 mM Tris-HCl (pH 7.5)–5 mM sodium azide (TA buffer), incubated with 1/2 volume of rabbit anti-mouse IgG (Pierce) at 4°C for 25 min, washed once with TA buffer, and incubated with 30 μg of H6.1 MAb for 2 h at 4°C. After being washed three times in TA buffer, the beads were used for V-ATPase immunoprecipitation. Approximately 1 mg of cellular protein in 500 μl of precleared extract was used per 30 μl of immunobeads for immunoprecipitation. Extracts (equal amounts of cellular protein) were incubated with immunobeads for 2 h at 4°C with rotation. Then immunocomplexes were washed three times with TA buffer supplemented with 1 mM EGTA, 1 mM phenylmethylsulfonyl fluoride, 40 μg of leupeptin/ml, 5 μg of aprotinin/ml, and 1 μg of pepstatin/ml. For Western blot analysis, the immune complexes were resuspended in Laemmli sample buffer and incubated at 95°C for 5 min and after centrifugation, the supernatant was used for sodium dodecyl sulfate-polyacrylamide gel electrophoresis (SDS-PAGE) followed by electroblotting onto a polyvinylidene difluoride membrane. Immunodetection of a and E subunits was performed with equal protein amounts of the immunoprecipitates with pan-a (V_o) polyclonal antibody and E-subunit (V_1)-specific MAb E11 (27), respectively. Membranes were washed three times and incubated with appropriate horseradish peroxidase-conjugated secondary antibody. The immunocomplexes were visualized by chemiluminescent detection with the Phototope Western Detection system (Cell Signaling Technology). The images were digitalized with the Alpha Ease FluorChem digital imaging system (Alpha Innotech Corp., San Leandro, Calif.). The optical density of the bands was quantified. In this assay, the ratio of subunit a to subunit E was used as an index of V-ATPase assembly.

For the enzymatic assay, V-ATPase was immunoprecipitated as described above and the ATPase activity was assayed directly on the bead immunoprecipitates as previously described (21). Briefly, aliquots of the immunoprecipitate were preincubated in the presence or absence of a V-ATPase inhibitor (200 nM concanamycin A or 1 mM *N*-ethylmaleimide). The reaction was initiated by addition of 3 mM ATP. After 30 min, the reaction was stopped by addition of trichloroacetic acid. Chloroform extraction was performed to remove lipids and detergents. ATP hydrolysis was estimated by a spectrophotometric measurement of inorganic phosphate.

Measurement of ATP and ADP content. Cellular ATP was measured by using an ATP bioluminescence assay (Roche assay kit CLS II), using the protocol of the manufacturer, with modification to measure ADP. After the experimental treatments, cell extracts were prepared by boiling in 200 mM Tris–8 mM EDTA (pH 7.75). Then ATP was determined by adding luciferin/luciferase by automated injection in a luminometer (Optocomp II; MGM Instruments, Hamden, Conn.) with integration of the light signal for 2 s. The ATP concentration was calculated from a standard curve. For the measurement of the sum of ATP and ADP, ADP was converted to ATP by incubation of aliquots of the same extracts with pyruvate kinase (0.05 U/100 μl) in the presence of an excess of phosphoenolpyruvate (50 μM) for 30 min as described previously (18). Cellular protein content was determined by using the BCA protein assay. The ATP and ADP contents were expressed as picomoles per microgram of protein.

V-ATPase traffic assay by cell surface biotinylation. The method used for cell surface biotinylation is a modification of a published procedure (25). HK-2 cells were subjected to control or experimental conditions and then kept on ice throughout the experiment. Cells were washed three times with ice-cold PBS-CM (PBS with 1 mM $MgCl_2$ and 0.1 mM $CaCl_2$) and incubated for 15 min with 1.5 mg of EZ-Link Sulfo-NHS-LC-Biotin (Pierce)/ml in ice-cold biotinylation buffer (10 mM triethanolamine, 2 mM $CaCl_2$, 150 mM NaCl [pH 9.0]) with gentle shaking. Then the cells were washed once with quenching buffer (192 mM glycine and 25 mM Tris in PBS-CM) and incubated for an additional 10 min in quenching buffer. Cells were then rinsed twice with PBS-CM, scraped into ice-cold buffer containing 50 mM Tris-HCl (pH 7.6), 120 mM NaCl, 1% Nonidet P-40, 10% glycerol, 1 mM phenylmethylsulfonyl fluoride, 2 mM sodium orthovanadate, 10 mM sodium pyrophosphate, 40 μg of leupeptin/ml, 5 μg of aprotinin/ml, 1 μg of pepstatin/ml, 100 mM NaF, 1 mM EDTA, and 1 mM EGTA. After lysis on ice for 60 min, extracts were centrifuged for 10 min at 14,000 × *g* at 4°C. The protein concentration of the supernatants was measured, and 500 μg of protein in 200 μl of lysis buffer was transferred to new tubes. After addition of 50 μl of a 50% slurry of streptavidin-agarose beads, the tubes were rotated for 2 h at 4°C. An aliquot of the supernatant was retained for determination of total subunits a and B. Beads were collected by brief centrifugation, and the supernatants were collected to represent the unbound intracellular pool. The beads were washed three times with 20 mM HEPES (pH 7.5)–150 mM NaCl–10% glycerol–0.1% Triton X-100, and the biotinylated proteins were eluted by boiling in Laemmli sample buffer for 5 min. Proteins of the supernatants were resolved by SDS-PAGE and immunoblotted with antibodies for subunits a and B1 as described above.

Assays of phosphorylation of protein kinases Akt and p70 S6. HK-2 or LLC-PK_1 cells were serum starved overnight prior to the experiments. To block PI3K, cells were pretreated for 60 min with 25 μM LY294002 prior to any stimulation. After stimulation or infection with Adeno/Myr-p110-Myc or Adeno/LacZ for the periods of time indicated in Results, cell lysates were prepared as described in the previous section. Twenty micrograms of protein of the total cell extract was resolved by SDS-PAGE and electroblotted onto a polyvinylidene difluoride membrane. Membranes were blocked in 10 mM Tris (pH 7.5)–100 mM NaCl–0.1% Tween 20 containing 5% nonfat dry milk, followed by incubation with primary antibody against Akt phosphorylated on Ser473 and antibody against total Akt (phosphorylation state independent) and phosphorylation-state-independent and phosphospecific p70 S6 kinase antibodies (phospho-p70 S6 kinase [Thr389] and p70 S6 antibodies) (Cell Signaling Technology). Membranes were washed three times and incubated with appropriate horseradish peroxidase-conjugated secondary antibody. The immunocomplexes were visualized and analyzed by densitometry as described above. The level of phosphorylated protein kinases was normalized to the level of total kinase and used as a marker of its activation.

Immunofluorescent staining of V-ATPase and confocal microscopy. HK-2 or LLC-PK_1 cells were plated on coverslips, grown to 60 to 75% confluence, and treated under control or experimental conditions as indicated in Results. Coverslips were rinsed three times with PBS. Then cells were fixed in 4% (wt/vol) paraformaldehyde in PBS. After three PBS rinses, the aldehyde groups were quenched for 10 min in 50 mM NH_4Cl. Then, after three PBS rinses, cells were permeabilized in 0.1% Triton X-100 in PBS for 10 min and again rinsed three times with PBS. Coverslips were blocked with 20% calf serum–1% polyethylene glycol (molecular weight, 20,000) in PBS for 30 min. For V_1 staining, the HK-2 cells were incubated with E11 antibody (hybridoma supernatant diluted 1:5 in blocking buffer) overnight at 4°C. After three PBS rinses, the coverslips were incubated with fluorescein isothiocyanate (FITC)-labeled donkey anti-mouse IgG (Jackson ImmunoResearch Laboratories, Inc., West Grove, Pa.) (1:50) for 45 min. For V_1 staining, the cells were incubated with polyclonal rabbit B1 antibody (1:250 in blocking buffer) overnight at 4°C. After three PBS rinses, the coverslips were incubated with Texas red-conjugated donkey anti-rabbit IgG (1:50) (Jackson ImmunoResearch Laboratories, Inc.). After three final PBS rinses, the coverslips were mounted with 50% glycerol–1 mM *p*-phenylenediamine in PBS with or without 4′,6′-diamidino-2-phenylindole (DAPI) (1.5 μg/ml) to counterstain nuclei. For V_o staining, the HK-2 cells were incubated with polyclonal rabbit pan-a antibody (1:250 in blocking buffer) overnight at 4°C. After three PBS rinses, coverslips were incubated with FITC or Texas red-conjugated donkey anti-rabbit IgG (1:50) (Jackson ImmunoResearch Laboratories, Inc.) for 45 min and mounted as indicated. For whole V-ATPase staining, the LLC-PK_1 cells were incubated overnight with protein A-agarose-purified H6.1 MAb (5 μg/ml of blocking buffer) at 4°C with subsequent incubation, after

three PBS rinses, with FITC-labeled donkey anti-mouse IgG (Jackson ImmunoResearch Laboratories, Inc.) (1:50) for 45 min.

For double-label immunofluorescent staining, coverslips were incubated first with polyclonal rabbit a antibody (1:250 in blocking buffer) overnight at 4°C. After three PBS rinses, coverslips were incubated with Texas red-conjugated donkey anti-rabbit IgG (1:50) for 45 min. Next, coverslips were incubated with E11 antibody (nondiluted hybridoma supernatant) for 1 h. After three PBS rinses, coverslips were incubated with FITC-labeled donkey anti-mouse IgG (1:50) for 45 min and, after three PBS rinses, mounted as indicated. As a negative control, the first antibody was omitted and cells were incubated with blocking buffer alone. "Crossover " of the fluorescent signal (rodamine fluorescence in the fluorescein filter and fluorescein fluorescence in the rodamine filter) was used as a further means of control. The slides were examined with the 60× oil immersion objective of a 1024 ES laser scanning confocal microscope equipped with LaserSharp image acquisition and analysis software (Bio-Rad). Series of Z sections were collected with a 0.30- to 0.50-μm Z-step. Alternatively, an epifluorescence Nikon TE300 microscope equipped with the MicroPublisher Imaging system (Qimaging, Burnaby, British Columbia, Canada) was used.

Detection of acidic intracellular compartments. To visualize acidic intracellular compartments and V-ATPase-dependent acidification, we used the acidic pH probe 3-(2,4-dinitroanillino)-3′-amino-*N*-methyldipropylamine (DAMP) (Molecular Probes, Eugene, Oreg.). Cells growing on coverslips were incubated for 60 min in culture medium containing 50 μM DAMP. Fixation and permeabilization were as described above. After blocking, the cells were incubated with antidinitrophenyl polyclonal antibody conjugated to fluorescein (1:50) (Molecular Probes) overnight at 4°C. After three final rinses with PBS, coverslips were mounted and examined as described above. Image analysis was performed using NIH-Scion Image software (v 4.0). The average fluorescence intensities in rectangular areas containing DAMP-positive structures and fluorescence intensity profiles (distribution of the fluorescence along the cross section line in the region of interest) were quantitated. For each sample, 18 to 24 cells from three or four randomly chosen fields were analyzed.

Statistical analysis. Data were analyzed by the unpaired *t* test or Mann-Whitney U test.

RESULTS

Glucose-dependent acidification of intracellular compartments by V-ATPase. The acidic pH probe DAMP easily penetrates through the plasma membrane and accumulates in the cellular compartments with low pH (usually, pH < 6.0). Following chemical fixation, which does not affect the probe distribution, DAMP can be specifically detected with antidinitrophenol antibody (1). In renal tubular epithelial cells, DAMP was colocalized with V-ATPase, and all acidic compartments identified with DAMP were also stained with V-ATPase antibody H6.1 (64). Therefore, DAMP staining may be used to detect V-ATPase-dependent acidic pools. DAMP labeling of LLCPK (Fig. 1a, upper panels) or HK-2 (Fig. 1a, lower panels) cells maintained in normal growth medium containing glucose showed scattering bright vesicles, sometimes localized asymmetrically around nuclei. Most of them disappeared after overnight incubation in glucose-free medium containing dialyzed serum and 0.1 mM glucose. The intensity of the fluorescence of DAMP-positive structures was also decreased (Fig. 1b; see also Fig. S3a in the supplemental material). Stimulation with 25 mM glucose for 15 min before DAMP addition restored the number, appearance, and fluorescence intensity of acidified vesicles seen in control conditions. In contrast, incubation with the same concentration of the osmotic agent D-mannitol did not produce a noticeable effect on the DAMP accumulation. (Fig. 1a, upper panels; see also Fig. S3a in the supplemental material). This excludes the possibility that the effect of glucose was related to an increase in osmolarity. Pretreatment of cells for 60 min with 100 nM concanamycin A, a highly specific inhibitor of V-ATPase (5), or with 25 μM LY294002, a widely used inhibitor of PI3K, totally eliminated the manifestation of the glucose stimulation and did not affect the nonstimulated cells (Fig. 1a, lower panels; see also Fig. S3a in the supplemental material). This demonstrates that glucose is required to

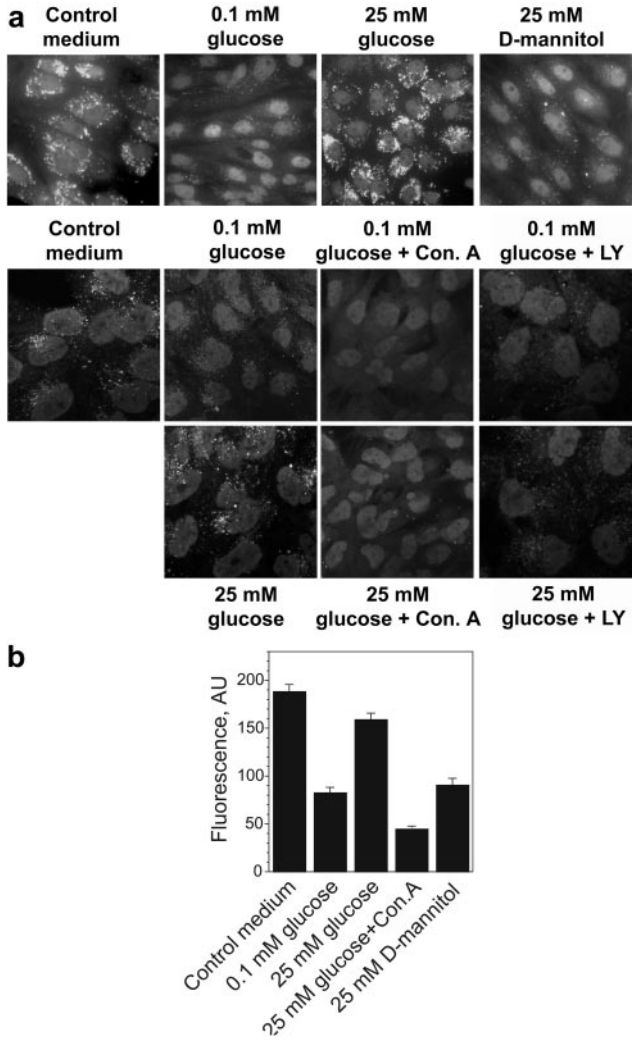

FIG. 1. V-ATPase-dependent, LY294002 (LY)-sensitive acidification of intracellular compartments of renal epithelial cells in response to glucose deprivation/stimulation. HK-2 cells (a) or LLC-PK_1 cells (a and b) were incubated in standard medium containing serum and glucose on coverslips. Sixteen to eighteen hours prior to the experiment cells were transferred to glucose-free medium containing dialyzed serum and 0.1 mM glucose. Concanamycin A (Con. A) (100 nM), LY294002 (25 μM), and vehicle were added 60 min before stimulation with glucose or D-mannitol (25 mM). Cells were labeled with DAMP, fixed, and stained with fluorescein-conjugated antidinitrophenol antibody. (a) Bright fluorescent structures are acidic compartments. (Upper panels) Acidification of intracellular compartments is induced by glucose but not by the same concentration of D-mannitol. (Lower panels) LY294002 and concanamycin A prevent the effect of glucose. Results shown are representative of five independent experiments. (b) Analysis of fluorescence intensity in LLC-PK_1 cells labeled with DAMP. Image analysis of the average fluorescence intensities in cytoplasmic rectangular areas and fluorescence intensity profiles of cross-sections (see Fig. S3 in the supplemental material) were performed using NIH-Scion Image software. Average fluorescence (mean ± standard error of the mean, arbitrary units [AU]) for 18 to 24 cells from three or four randomly chosen fields is shown.

maintain the low pH in intracellular compartments of cultured proximal tubular cells. It is likely that glucose stimulates acidification of the vesicular/vacuolar system by V-ATPase, and this process requires active PI3K.

Glucose-dependent assembly and trafficking of V-ATPase in renal tubular epithelial cells. The reversible dissociation of the V_1 and V_o domains in response to a change of extracellular nutrients, such as glucose abundance, is a well-characterized regulatory mechanism in yeast and some insect cells (30, 31, 63). Because V-ATPase is a very ancient enzyme in eukaryotic cells, a similar mechanism of the response to glucose could be expected in our model system. We immunoprecipitated V-ATPase holoenzyme from lysates of LLC-PK_1 cells containing 3-[(3-cholamidopropyl)dimethylammonio]-1-propanesulfonate (CHAPS) and nonylglucoside with the V_1-specific monoclonal antibody H6.1. This antibody recognizes the E subunit and has been successfully used previously to immunoprecipitate the active pump and to stain V-ATPase in LLC-PK_1 cells (21, 64). The a subunit (in V_o) and the E subunit (in V_1) were detected in H6.1 immunoprecipitates by immunoblotting with polyclonal antibody to subunit a and E11, another monoclonal antibody for the E subunit. The a/E ratio was used as a measure of the assembly of V_o and V_1 domains.

Incubation of LLC-PK_1 cells in medium deprived of glucose and serum for 16 h significantly diminished coprecipitation of subunit a with subunit E, indicating disassembly of V-ATPase (Fig. 2a and c). Serum deprivation alone also diminished the amount of assembled V-ATPase detected in immunoprecipitates, but the contribution of glucose seemed to be greater (Fig. 2b). Treatment of LLC-PK_1 cells with 10 mM glucose for 15 min induced an increase in V-ATPase assembly (Fig. 2a to c). The effect of glucose was mimicked by 2-deoxyglucose (Fig. 2a), a glucose analog which is phosphorylated by cytoplasmic hexokinase but cannot be metabolized further in the glycolytic pathway (15). The same effect was observed when glucose was combined with 2-deoxyglucose. These results show that glucose metabolism beyond the hexokinase step is not required to induce assembly of the V_1 and V_o domains of V-ATPase. This suggests that another glucose-induced signal may be responsible for V-ATPase assembly. LY294002 attenuated the effect of glucose on V-ATPase assembly (Fig. 2b and c). These data suggest that stimulation of V-ATPase assembly in response to glucose is mediated by PI3K-dependent signaling. Glucose deprivation resulted in a significant decrease in the concanamycin A-sensitive ATP hydrolytic activity of immunoprecipitated V-ATPase. Cell stimulation with glucose for 15 min restored the ability of immunoprecipitated V-ATPase to hydrolyze ATP. The effect of glucose was prevented by pretreatment with LY294002 (Fig. 2d).

In order to test how glucose availability in our model affected the steady-state level of intracellular ATP, we determined the cellular content of ATP and ADP in time course and dose-response experiments. As expected, 16 h of serum and glucose starvation resulted in a dramatic decrease in the concentration of ATP and in the ATP/ADP ratio (Fig. 2e). Hence, ATP availability can be a potential contributing factor in V-ATPase disassembly and in the decrease in activity seen after chronic glucose deprivation. However, cell treatment with 10 mM glucose for 15 min, which was sufficient to stimulate V-ATPase assembly and activity, did not restore the steady-state level of ATP to the control level. Elevation of the glucose concentration to 25 mM or prolongation of the stimulation to 30 min produced some increase in the ATP/ADP ratio and steady-state level of intracellular ATP (Fig. 2e). These results suggest that substrate availability is not a primary regulatory mechanism in V-ATPase assembly and activation in response to glucose.

To further characterize V-ATPase assembly and to test whether glucose affects V-ATPase trafficking in renal tubular cells, we performed an immunofluorescence study using antibody H6.1 to V-ATPase holoenzyme, antibodies to subunits B1 and E (E11) (V_1 domain), and antibody to the a subunit (V_o domain). As shown previously (64), the H6.1 antibody is optimally suitable for immunostaining of V-ATPase in LLC-PK_1 cells. When cultured in standard medium, these cells show clear vesicular localization of V-ATPase but no apparent plasma membrane staining (Fig. 3a), which is consistent with previous observations (64). The vesicles are scattered throughout the cytoplasm or sometimes clustered asymmetrically in a perinuclear area. V_o staining with pan-a antibody displayed similar localization. In some vesicles it was colocalized with V_1 staining (shown in yellow on overlaid images), suggesting assembly of V_1 and V_o domains of V-ATPase (Fig. 3a). HK-2 cells also had V-ATPase detectable by immunofluorescence (Fig. 3b). H6.1 antibody does not bind to human V-ATPase; therefore, the subcellular distribution of V_1 and V_o domains of V-ATPase in HK-2 cells was studied using E11 and pan-a antibodies. The pattern of staining indicates mostly vesicular/vacuolar localization of V-ATPase, but diffuse E11 staining also suggests cytoplasmic localization of V_1. In some cases, true colocalization of V_1 and V_o domains can be detected (yellow spots) (Fig. 3b). In contrast to the LLC-PK_1 cells, the plasma membrane and/or perimembrane area of HK-2 cells, which retain more differentiated features of the proximal tubular epithelial cells, was distinctly stained with both V-ATPase antibodies (Fig. 3b). Confocal vertical (XZ) sections showed that in some cases V-ATPase, especially the V_o domain, is localized predominantly on the apical pole of the cell (Fig. 3b and Fig. 4c, control), suggesting that localization of V-ATPase in these cells is polarized. In proximal tubular cells in situ, V-ATPase is concentrated in numerous vesicles of the subapical band of the brush border (8). Thus, studies of localization and colocalization of the V_1 and V_o domains suggest that the cellular pool of V-ATPase under normal culture conditions may consist of both assembled and disassembled enzyme.

Glucose deprivation or replacement dramatically changed the patterns of V-ATPase staining in both cell lines. Untreated cells showed clear and bright vesicular/vacuolar staining of V-ATPase with H6.1 antibody (Fig. 4a, arrowheads). Glucose deprivation of LLC-PK_1 cells decreased the localization of the V_1 sector of V-ATPase in intracellular structures as well as its intensity (Fig. 4a). The more diffused and uniform H6.1 staining suggests an increase in cytoplasmic localization of V_1 (Fig. 4a, insets, arrows). Stimulation with glucose, but not with D-mannitol, quickly restored vesicular/vacuolar staining of V-ATPase (Fig. 4a, arrowheads), decreasing diffuse cytoplasmic staining (Fig. 4a, insets). These results are consistent with the dissociation of V_1 from the membrane and diffusion to the cytoplasm in response to glucose deprivation and reassociation following glucose replacement. Glucose-dependent vesicular

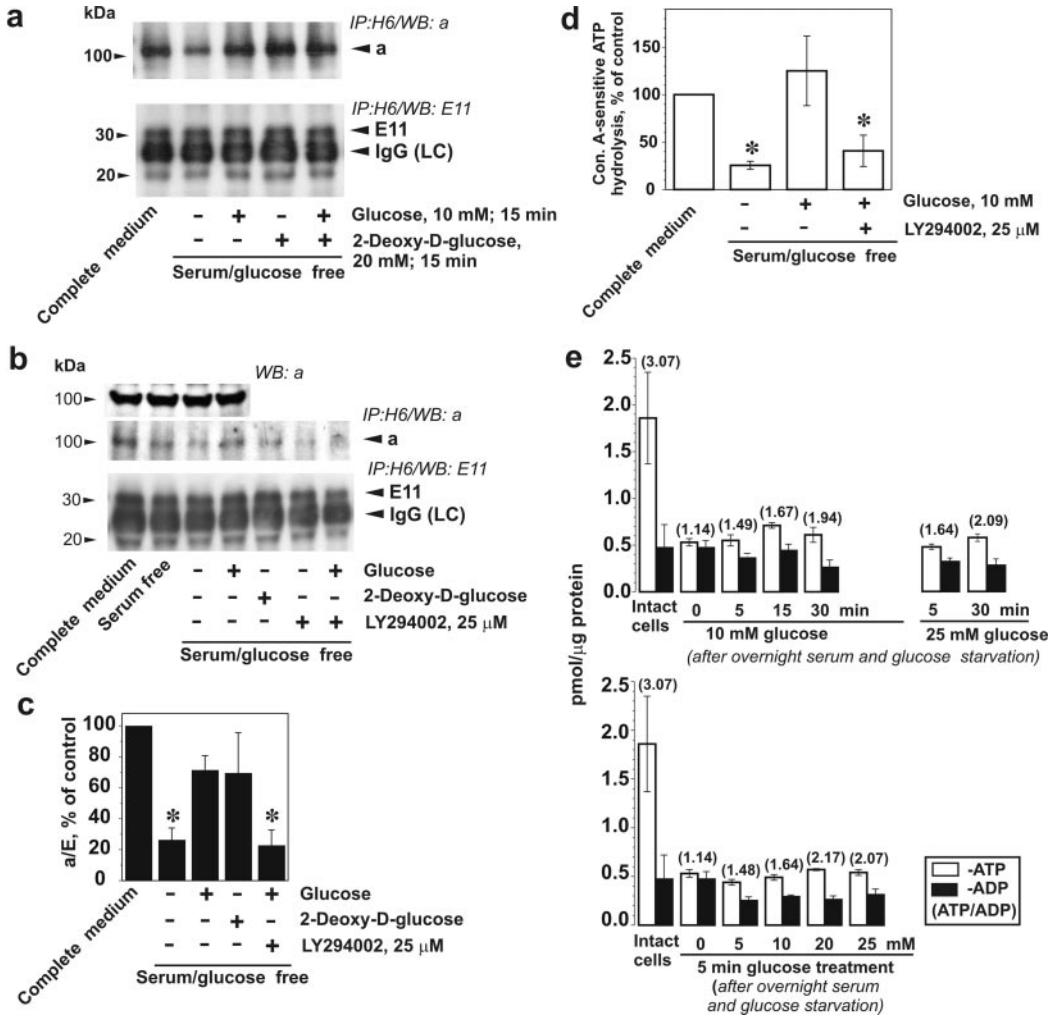

FIG. 2. Glucose stimulates V-ATPase assembly and ATP hydrolytic activity. LLC-PK1 cells were cultured to 70 to 80% confluence in 199 medium containing 10% FBS and 5.5 mM glucose. Prior to the experiments, cells were incubated in glucose-free DMEM overnight and were then stimulated with 10 mM glucose and/or 20 mM 2-deoxyglucose for 15 min. If the effect of PI3K inhibition was studied, LY294002 (25 μM) and vehicle were added 30 min prior to glucose addition. (a) After cell stimulation, V-ATPase was immunoprecipitated from the lysates with H6.1 MAb, which binds the V_1 domain on its E subunit. Coprecipitation of V_o and V_1 domains of V-ATPase was probed by Western blotting using antibodies against subunits a (V_o domain) and E (MAb E11, V_1 domain). The amount of a subunit present in the immunoprecipitate decreased after glucose and serum deprivation and was quickly restored by cell stimulation with glucose. Glucose-induced increase of subunit a coprecipitated by V_1-specific antibody (upper panels) without changes in the amount of detected E subunit (lower panels) indicates an increase in V-ATPase assembly. (b) Effect of glucose on V-ATPase assembly is attenuated by PI3K inhibitor LY294002. (Top panels) Immunoblot detection of a subunit in the cell lysates after glucose deprivation and replacement before V-ATPase immunoprecipitation. No changes were observed. Glucose-stimulated increase of subunit a and E coprecipitation was prevented by preincubation of cells with 25 μM LY294002 (second and third panels from the top). (c) Densitometric analysis of the a/E ratio. Data are presented as percentages of the control (untreated cells). Shown are means ± standard errors of the means ($n = 3$ or 4); *, $P < 0.05$ (Student's t test) versus results for the glucose-treated group. (d) Concanamycin A (Con. A)-sensitive ATP hydrolysis by immunoprecipitated V-ATPase from LLC-PK_1 cells after glucose deprivation/replacement. V-ATPase was immunoprecipitated from cell lysates with H6.1 antibody. After preincubation of aliquots of the immunoprecipitate in the presence or absence of a V-ATPase inhibitor (200 nM concanamycin A or, alternatively, 1 mM *N*-ethylmaleimide [NEM]), 3 mM ATP was added to start the reaction. After 30 min, the reaction was stopped and ATP hydrolysis was estimated by spectrophotometric measurement of inorganic phosphate. Ninety to ninety-five percent of the ATP hydrolytic activity in immunoprecipitates was concanamycin A/NEM sensitive (0.25 to 3.1 nmol of P_i/min/mg of cell protein in untreated cells). Data are presented as percentages of the control (untreated cells) as means ± standard errors of the means ($n = 3$); *, $P < 0.05$ (Student's t test) versus results for the glucose-treated group (e) Effect of glucose deprivation/stimulation on the levels of ATP and ADP and the ATP/ADP ratio. Cells were grown in complete medium. Prior to glucose treatments, cells were deprived overnight of serum and glucose. The cells were then incubated with 5 to 25 mM glucose for various periods of time up to 30 min, and cell extracts were prepared. ATP and ADP determination was performed as indicated in Materials and Methods. Data are presented as means ± standard errors of the means for three independent experiments performed in triplicate.

trafficking can also contribute to the changes in the pattern of V-ATPase staining. Pretreatment of cells with LY294002 prevented the effect of glucose, suggesting that PI3K mediates the effect of glucose on V-ATPase trafficking. Untreated HK-2 cells showed both vacuolar and plasma membrane and/or perimembrane localization for V_1 subunits E and B1 (Fig. 4b and c, arrowheads). V_o staining with pan-a antibody showed localization of the a subunit on the plasma membrane (arrowheads)

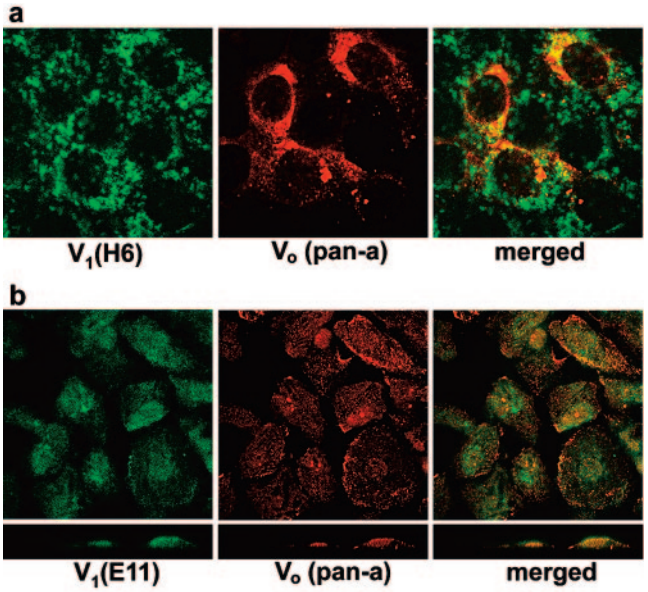

FIG. 3. Localization of V_1 and V_o domains of V-ATPase in renal tubular epithelial cells. LLC-PK_1 (a) and HK-2 cells (b) were grown on coverslips in standard conditions and were then fixed and permeabilized followed by double staining with antibodies against V_1 (H6.1 or E11) and V_o (pan-a) subunits as described in Materials and Methods. Confocal images (0.5-μm optical sections) are shown with overlays (merged) of two stainings, as well as lateral views (XZ vertical section) (b, lower panels).

and small vesicles. Glucose removal induced a loss of vacuolar (E) and plasma membrane (B1) staining for subunits of the V_1 domain. In addition, V_o staining with pan-a disappeared from the plasma membrane and moved to the large vacuoles (arrows). Replacement of glucose resulted in recovery of the staining patterns for the E, a, and B subunits seen in the control. This effect of glucose was eliminated by pretreatment with LY294002, and the staining pattern was similar to that seen under glucose-deprived conditions. LY294002 did not induce apparent changes in the staining of nonstimulated cells (results not shown). The pattern of double staining of subunits a and E in the presence or absence of glucose is shown in Fig. 4c. Glucose removal significantly changed the pattern of localization of the V_1 and V_o subunits. Polarized localization of V-ATPase on the apical pole of the cell could be observed only in the presence of glucose.

In order to confirm that glucose can induce the trafficking of V-ATPase from the intracellular membranes to the plasma membrane, we performed cell surface biotinylation. The biotinylated proteins were precipitated on streptavidin beads followed by immunoblot analysis of V_o and V_1 subunits in biotinylated (surface) and nonbiotinylated (intracellular) fractions. Subunit a of the V_o domain has transmembrane domains and several extracellular loops (43) potentially accessible for cell surface biotinylation. HK-2 cell lysates precipitated with streptavidin beads after biotinylation performed at 0°C contained a small but still detectable amount of a and B subunits (Fig. 5). The presence of V_1 subunit B among the biotinylated proteins is another piece of evidence that the plasma membrane contains assembled V-ATPase. Glucose deprivation diminished the a-subunit content in the biotinylated fraction, whereas glucose replacement for 15 min induced a noticeable increase of the a-subunit content and a slight increase of the B-subunit content in the surface fraction. Densitometry confirmed a significant increase of the a subunit but not the B subunit in the biotinylated fraction (Fig. 5, lower panel). The effect of glucose was prevented by LY294002. These results provide further support that glucose induced PI3K-dependent trafficking of V-ATPase to the plasma membrane.

Stimulatory effect of constitutively active p110α subunit of PI3K on acidification of intracellular compartments by V-ATPase. To further investigate the role of PI3K in the control of V-ATPase trafficking and assembly, we characterized the effects of expression of the constitutively active form of this enzyme. The gene for chimeric protein Myr-p110-Myc, consisting of catalytic subunit p110α of PI3K ligated to a myristoylation signal sequence at its NH_2 terminus, was delivered to HK-2 and LLC-PK_1 cells with an adenoviral vector. As shown in Fig. 6, overnight incubation of both LLC-PK_1 (Fig. 6a) and HK-2 (results not shown) cells in the glucose-free medium containing 0.1 mM glucose and dialyzed serum resulted in almost complete disappearance of DAMP-labeled acidic compartments. Stimulation with 25 mM glucose for 15 min restored the number and the fluorescence intensity of DAMP-labeled acidic vesicles (Fig. 6b). This acidification was totally prevented by pretreatment with the inhibitor of V-ATPase concanamycin A (Fig. 6a) and with ammonium chloride (results not shown), a weak base commonly used to dissipate transmembrane proton gradients of any origin (22, 26). If cells were glucose deprived 48 h after infection with Adeno/Myr-p110-Myc but not Adeno/Lac-Z, the density and fluorescence intensity of DAMP-labeled vesicles were similar or greater than those in glucose-stimulated or control cells (Fig. 6; see also Fig. S3 in the supplemental material). DAMP accumulation in these compartments was eliminated by cell pretreatment with concanamycin A for 1 h (results not shown). DAMP accumulation induced by Myr-p110α expression was prevented by LY294002 (Fig. 6a, lower panel, and 6b). These results showed that the expression of the constitutively active catalytic subunit of PI3K is sufficient to maintain V-ATPase-dependent acidification of intracellular compartments in glucose-deprived conditions and the effect of the active PI3K is undistinguishable from glucose-induced stimulation.

Active p110α PI3K is sufficient to stimulate V-ATPase assembly and trafficking in glucose-deprived conditions. Next, we tested if the expression of active PI3K affects V-ATPase trafficking and assembly. The appearance of a diffuse cytoplasmic distribution of V-ATPase in LLC-PK_1 cells after glucose starvation (Fig. 7a, arrows) was prevented by adenoviral expression of Myr-p110α. V-ATPase was localized predominantly in compact bright vesicles. This was similar to untreated cells or cells stimulated after starvation with 25 mM glucose for 15 min (Fig. 7a, arrowheads). Control adenovirus Adeno/Lac-Z did not change the intracellular distribution of V-ATPase. In HK-2 cells, active PI3K dramatically changed the pattern of staining of V-ATPase in glucose-deprived cells and the effect of constitutively active PI3K exceeded the effect of glucose replacement (Fig. 7b). Both the V_1 (E and B) and the V_o (a) subunits were localized predominantly on the cell periphery near or on the plasma membrane and in distinct dense structures in perinuclear areas where V_1 and V_o were colocal-

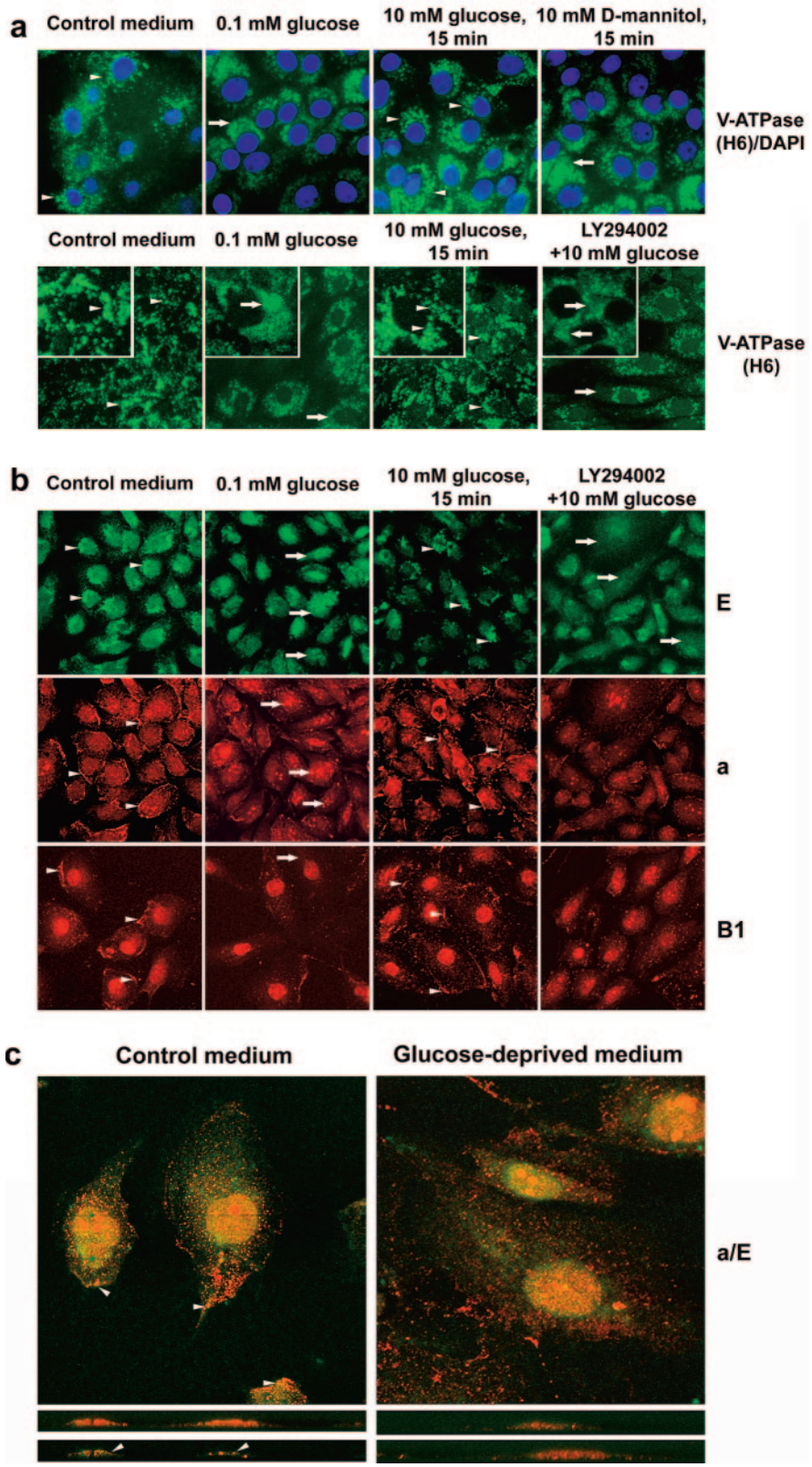

FIG. 4. Glucose-dependent, LY294002-sensitive translocation of V-ATPase in renal epithelial cells. (a) LLC-PK_1 cells were grown on coverslips in standard conditions. Prior to the experiments, cells were incubated in glucose-free DMEM overnight and were then stimulated with 10 mM glucose or 10 mM D-mannitol (upper panels) for 15 min. If the effect of PI3K inhibition was studied, LY294002 (25 μM) and vehicle were added 30 min prior to glucose addition. Then cells were fixed, permeabilized, and stained with H6.1 V-ATPase antibody. Nuclei were (upper panels) or were not (lower panels) counterstained with DAPI. In the presence of glucose (before glucose deprivation and after glucose replacement) bright

ized (Fig. 7b, arrowheads). PI3K also induced concentration and colocalization of V_1 and V_o domains in the subapical area and/or on the apical plasma membrane (Fig. 7b, a/E vertical). No significant changes in V-ATPase intracellular distribution were induced by expression of β-Gal.

Cell surface biotinylation experiments showed that adenoviral expression of p110α but not β-Gal is sufficient to increase the content of both the V_o (a subunit) and V_1 (B subunit) domains of V-ATPase in the biotinylated fraction of glucose-deprived cells (Fig. 8). The effect of p110 was prevented by LY294002 (Fig. 8b). The effect of the overexpression of active PI3K was similar to the effect of treatment with glucose. These results are consistent with the confocal imaging of vertical sections of HK-2 cells and provide further support to the notion that translocation of V-ATPase to the plasma membrane in response to glucose is mediated by PI3K-dependent signaling.

The data on coprecipitation of V_1 and V_o subunits in LLC-PK_1 cells presented above suggest that glucose stimulates assembly of V-ATPase holoenzyme via a PI3K-dependent signaling mechanism. To further confirm the involvement of PI3K in the stimulation of V-ATPase assembly, we examined the effect of constitutively active PI3K on the coprecipitation of a and E subunits in LLC-PK_1 cells (Fig. 9). V-ATPase immunoprecipitation with H6.1 antibody in LLC-PK_1 cells and subsequent immunoblot detection of a and E subunits showed that glucose-deprived cells infected with Adeno/Myr-p110-Myc contained more assembled V-ATPase, estimated by the a/E ratio, than cells infected with Adeno/LacZ or noninfected glucose-deprived cells (Fig. 9a and c). Active PI3K restored most of the assembled V-ATPase observed in untreated cells growing under standard conditions (Fig. 9a). LY294002 attenuated the effect of Myr-p110α expression (Fig. 9b and c). These results are consistent with results of experiments on glucose stimulation after pretreatment with the PI3K inhibitor LY294002 (Fig. 2).

Rapid activation of PI3K-dependent signaling in renal epithelial cells by glucose. To check the effect of glucose on PI3K-dependent signal transduction in renal epithelial cells, we analyzed the responses of protein kinases Akt and p70 S6K to glucose. In most systems, these enzymes are crucial downstream mediators of PI3K signals. In response to activation of PI3K, both Akt and p70 S6K are activated by phosphorylation via intermediate phosphatidylinositol 3-phosphate-dependent protein kinase-1 (PDK1) (3, 13, 60). Stimulation of glucose- and serum-deprived HK-2 cells with glucose, over a range of 5 to 20 mM, induced a rapid progressive increase in phosphorylation of Akt on Ser^{473} (Fig. 10A) and phosphorylation of p70 S6K on Thr^{389} (Fig. 10B). Activation of Akt phosphorylation was distinct within 2.5 min after glucose addition and reached more than a threefold increase after 5 to 15 min, as determined by densitometry (data not shown). The increase in phosphorylation of p70 S6K on Thr^{389} was more than 10-fold after 5 min (densitometry; data not shown) and continued to increase over the next 25 min. Pretreatment of cells with 25 μM LY294002 totally abolished stimulation of the phosphorylation of both protein kinases. Similar results were obtained with LLC-PK1 cells (data not shown). These results demonstrate that, in renal proximal tubular cells, glucose induced rapid high-amplitude activation of PI3K-dependent signaling.

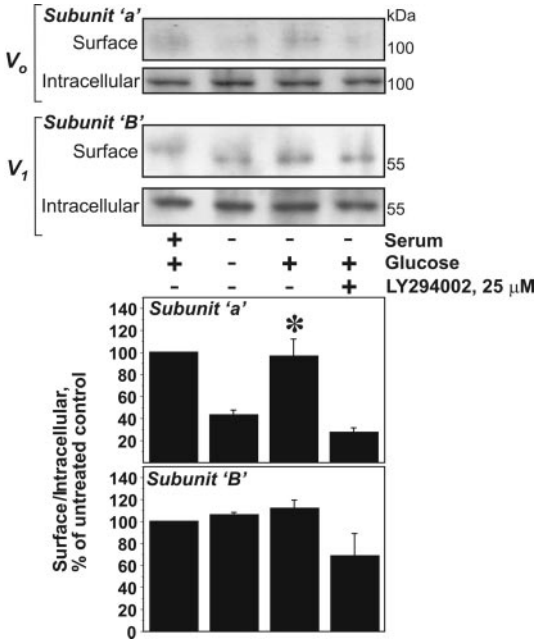

FIG. 5. Glucose-induced increase in cell surface pool of V-ATPase in HK-2 cells. Subconfluent HK-2 cells were incubated in glucose-free DMEM overnight and were then stimulated with 10 mM glucose for 15 min. If the effect of PI3K inhibition was studied, LY294002 (25 μM) and vehicle were added 30 min prior to glucose addition. Then cell surface biotinylation was performed on ice, as described in Materials and Methods. Biotinylated proteins representing the cell surface pool were precipitated on streptavidin beads. Nonbiotinylated (intracellular) proteins remained in the supernatant. Both fractions were probed by immunoblotting with antibodies against a (V_o) and B1 (V_1) subunits. Results shown are representative of four independent experiments. (Lower panel) Densitometric analysis of the surface V-ATPase/intracellular V-ATPase ratio. Data are presented as percentages of the control (untreated cells) as means ± standard errors of the means (n = 3 or 4); *, $P < 0.05$ (U-test) versus results for the glucose-deprived or LY294002-treated group.

DISCUSSION

The role of glucose in the control of V-ATPase activity and assembly is well described for the yeast *S. cerevisiae*, which

vesicular staining of V-ATPase is visible in the majority of cells (see arrowheads, for example). Glucose deprivation induced appearance of diffuse staining (see insets, arrows, for example). (b) HK-2 cells were grown on coverslips in standard conditions. Prior to the experiments, cells were incubated in glucose-free DMEM overnight and were then stimulated with glucose with or without LY294002, as described above. Then cells were fixed, permeabilized, and stained with antibodies to V_1 subunits E and B1 and V_o subunit a. Vesicular staining of subunit E and peripheral perimembrane staining of B1 and a subunits in control conditions or after stimulation with glucose is seen (see arrowheads, for example). Glucose-deprived or LY294002-treated cells show more diffuse staining for the E subunit, disappearance of membrane staining for subunits a and B1, and translocation of subunit a to large vesicles (see arrows, for example). (c) Colocalization of a and E subunits in perimembrane and apical areas is observed only in the presence of glucose (arrowheads). Confocal images of optical 0.5-μM sections (upper panels) and vertical (XZ) sections (lower panels) are shown.

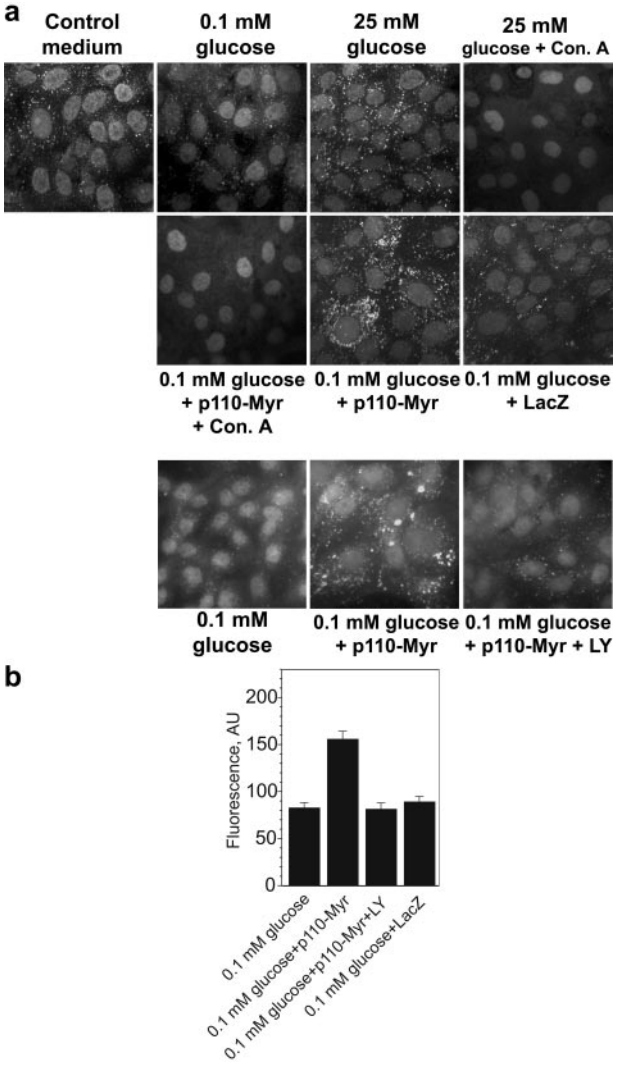

FIG. 6. V-ATPase-dependent acidification of intracellular compartments in renal epithelial cells expressing constitutively active PI3K. (a and b) LLC-PK_1 cells were incubated in standard medium containing glucose and serum on coverslips. Cells were infected with Adeno/Myr-p110-Myc or Adeno/LacZ at MOI 10 for 48 h. Sixteen to eighteen hours prior to DAMP labeling cells were transferred to glucose-free medium containing dialyzed serum and 0.1 mM glucose. Concanamycin A (Con. A) (100 nM) and 10 mM NH_4Cl were added 60 min before stimulation with glucose (25 mM). If the effect of PI3K inhibition was studied, LY294002 (LY) (25 μM) and vehicle were added 60 min prior to DAMP addition. Cells were labeled with DAMP, fixed, and stained with fluorescein-conjugated antidinitrophenol antibody. (b) Analysis of fluorescence intensity in LLC-PK_1 cells labeled with DAMP. Image analysis of the average fluorescence intensity in a cytoplasmic rectangular area and fluorescence intensity profiles of cross sections (see Fig. S3 in the supplemental material) was performed using NIH-Scion Image software. Average fluorescence (mean ± standard error of the mean, arbitrary units [AU]) for 18 to 24 cells from three or four randomly chosen fields is shown.

utilizes glucose as a preferred carbon source and a major growth factor. *S. cerevisiae* responds to glucose deprivation with rapid disassembly of V-ATPase into V_1 and V_o domains, and reassembly occurs after glucose replacement (30, 31). None of the glucose-sensing signaling mechanisms established for yeast cells are required to mediate the effect of glucose on V-ATPase assembly (44). V-ATPase in mammalian cells directly interacts with the glycolytic enzymes aldolase (35, 36) and phosphofructokinase-1 (54). This demonstrates not only functional but also spatial coupling of V-ATPase with glucose metabolism. However, due to the inherent complexity of mammalian systems, including glucose-sensing mechanisms, it was expected that the regulatory role of glucose in the control of V-ATPase function is not limited to the coupling of glycolysis and V-ATPase activity.

In this study, we show that glucose is a crucial factor for the control of V-ATPase in renal tubular epithelial cells. The effects of glucose are manifested at several levels: maintaining V-ATPase-dependent acidity of the vesicular system, translocation of the V-ATPase between intracellular compartments, reversible assembly of V_1 and V_o domains, and catalytic activity. We present evidence that glucose, besides providing substrates to maintain ATP pools, can stimulate V-ATPase via the PI3K signaling pathway.

Glucose withdrawal from both HK-2 and LLC-PK_1 cells prevented DAMP accumulation in the intracellular acidic compartments. Addition of glucose but not the osmotic agent D-mannitol quickly restored DAMP-positive acidic compartments. This process was eliminated by concanamycin A, a specific inhibitor of V-ATPase-dependent proton transport, and by disruption of transmembrane proton gradients with the weak base ammonium chloride. DAMP accumulation in response to glucose was also effectively prevented by the PI3K inhibitor LY294002. On the other hand, adenoviral expression of constitutively active PI3K was sufficient to maintain the abundance of DAMP-positive acidic compartments in glucose-deprived cells at least at the level observed in the untreated control. Inhibition of V-ATPase or PI3K abolished the effect of constitutively active PI3K. Taken together, these data show that glucose stimulates the pumping of protons by V-ATPase into intracellular acidic compartments and the effect of glucose is mediated by PI3K. DAMP immunocytochemistry does not allow the identification of particular intracellular compartments with low pH (the Golgi apparatus, secretory vesicles, endosomes, or lysosomes) involved in the response to glucose. Further experiments are required to address this question. Our results are consistent with published observations. Glucose was reported to induce an increase in cytoplasmic pH in mouse pancreatic islets (50). Glucose elicited a bafilomycin-sensitive pH decrease in secretory granules in insulin-secreting cells, but the signaling pathway linking glucose and V-ATPase was not established (57). Wortmannin has been reported to affect the morphology and recycling of endosomes and lysosomes (38), but the effects of glucose were not addressed in that study. The present study demonstrates for the first time the following sequence of events: glucose→PI3K →activation of V-ATPase→ acidification of intracellular compartments.

Glucose-induced acidification of intracellular compartments by V-ATPase was accompanied by extensive translocation of the V_1 and V_o domains between different cellular compartments. Untreated cells showed distinct vesicular membrane staining (LLC-PK_1) or both vesicular and plasma membrane staining (HK-2) with V-ATPase antibodies. In control conditions, the V_1 and V_o domains of V-ATPase were partially colocalized and, presumably, assembled. Coprecipitation of subunits from the V_1 and V_o domains confirmed the presence

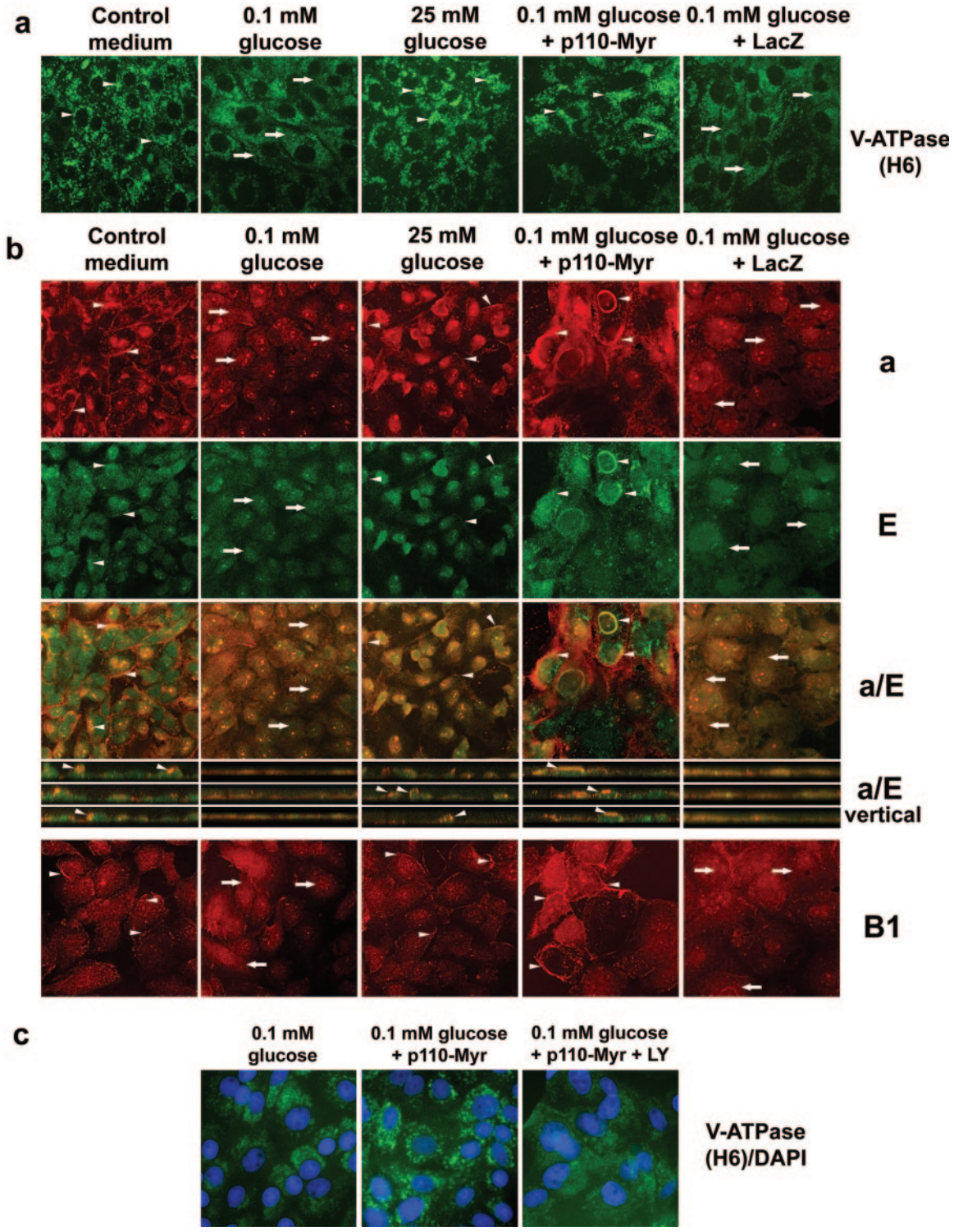

FIG. 7. Translocation of V-ATPase in renal epithelial cells overexpressing constitutively active PI3K. (a) LLC-PK_1 cells were incubated in standard medium containing glucose and serum on coverslips. Cells were infected with Adeno/Myr-p110-Myc or Adeno/LacZ at an MOI of 10 for 48 h. Then cells were transferred to glucose-free medium containing dialyzed serum and 0.1 mM glucose for 16 to18 h followed by stimulation with 25 mM glucose for 15 min. Then cells were fixed, permeabilized, and stained with H6.1 V-ATPase antibody. Expression of constitutively active PI3K was sufficient to maintain vesicular staining of V-ATPase in glucose-deprived cells, similarly to cells incubated in standard medium or after stimulation with glucose (see arrowheads, for example). (b) HK-2 cells were grown on coverslips in standard conditions. Infection with Adeno/Myr-p110-Myc and Adeno/LacZ, serum deprivation, and stimulation were as described above. Cells were fixed, permeabilized, and double stained with antibodies for V_1 subunit E and V_o subunit a or stained with antibody against V_1 subunit B_1. Confocal images of a and E double staining (0.5-μm optical sections) are shown together with overlays of two stainings (a/E). Overlaid images of vertical (XZ) sections for a/E double staining are also shown. (c) LLC-PK_1 cells were incubated in standard medium containing glucose and serum on coverslips. Infection with Adeno/Myr-p110-Myc and Adeno/LacZ, serum deprivation, and stimulation were as described above. LY294002 (LY) (25 μM) and vehicle were added 60 min prior to cell fixation. Then the cells were fixed, permeabilized, and stained with H6.1 V-ATPase antibody. Nuclei were counterstained with DAPI.

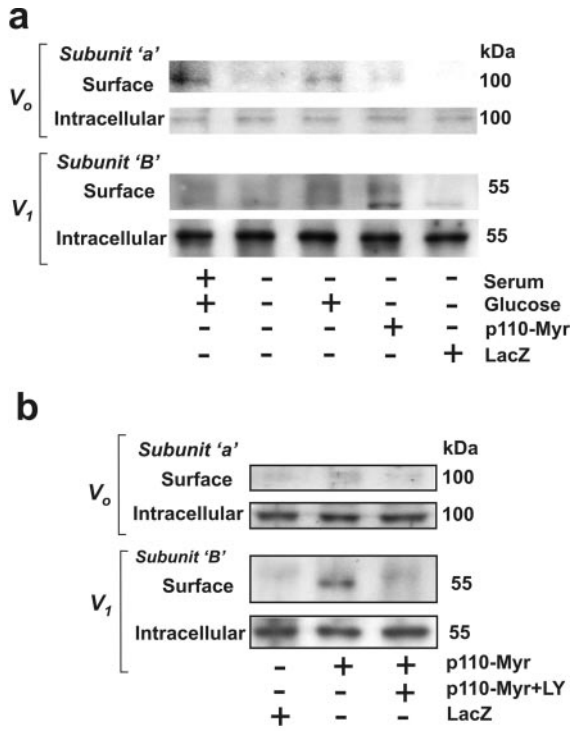

FIG. 8. Expression of constitutively active PI3K increases the cell surface pool of V-ATPase in HK-2 cells. Cells were grown in standard conditions. They were infected with Adeno/Myr-p110-Myc or Adeno/LacZ at an MOI of 10 for 48 h. Then cells were transferred to glucose- and serum-free medium for 16 to18 h followed by stimulation with 25 mM glucose for 15 min (a) or treatment with 25 μM LY294002 (LY) for 60 min (b). Then cell surface biotinylation was performed on ice. Cell surface (biotinylated) proteins were precipitated with streptavidin beads. Nonbiotinylated (intracellular) proteins remained in the supernatant. Both fractions were probed by immunoblotting with antibodies against a (V_o) and B1 (V_1) subunits. Results shown are representative of two independent experiments.

of the assembled holoenzyme in the untreated cells. Vertical sectioning of confocal images showed polarized apical localization of V-ATPase in HK-2 cells. Experiments with biotinylation of the cell surface provided evidence that at least part of the perimembrane V-ATPase is inserted in the apical plasma membrane. Glucose deprivation or replacement dramatically changed the pattern of V-ATPase localization. Glucose withdrawal induced the loss of membrane staining of V_o subunit a and V_1 subunit B1 and an increase in the staining of large intracellular vacuoles with pan-a antibody. In particular, in the absence of glucose we were unable to find any manifestations of polarized localization of V-ATPase in HK-2 cells. In addition, we observed an increase in diffuse staining with antibodies to subunits E and B1 in glucose-deprived cells. This suggests V-ATPase disassembly and diffusion of the V_1 domain into the cytoplasm. Analysis of coprecipitation of the V_1 and V_o domains confirmed V-ATPase disassembly. In most cases, these changes were quickly reversed by glucose replacement. The ability of glucose to restore control levels of V-ATPase assembly and activity as well as the pattern of subcellular localization was consistently demonstrated by immunoprecipitation, surface biotinylation, and immunofluorescent staining. These results suggest that glucose stimulates intracellular trafficking of membrane structures containing assembled pumps and disassembled V_o domains, as well as association of cytoplasmic V_1 with membrane-integrated V_o domains.

The effects of glucose on V-ATPase trafficking and assembly can be largely abolished by pretreatment with the PI3K inhibitor LY294002. On the other hand, they can be reproduced in glucose-deprived cells by adenoviral expression of the constitutively active catalytic subunit p110α of PI3K. Adenoviral delivery of the *lacZ* gene did not produce any noticeable changes in the pattern of the intracellular localization of V-ATPase. These results are consistent with DAMP immunocytochemistry and show that the effects of glucose are mediated by activation of PI3K.

The effects of glucose on V-ATPase assembly and trafficking are most likely independent of the metabolism of glucose in the glycolytic pathway and ATP level. This is suggested by two lines of experiments. First, 2-deoxyglucose, a glucose analog which is transported into the cytoplasm and phosphorylated by hexokinase but is not metabolized in the glycolytic pathway beyond this step, mimicked the effect of glucose on stimulation of V-ATPase assembly. Second, glucose replacement following starvation restored V-ATPase assembly earlier than the steady-state ATP level and ATP/ADP ratio. We observed only a partial and delayed recovery of ATP level and the ATP/ADP ratio after stimulation of glucose-deprived cells with glucose. The high demand for ATP in renal epithelial cells due to abundance of ATP-consuming ion pumps is well known. Slow and incomplete ATP recovery in renal epithelium after depletion experiments in vitro (12, 52) or renal ischemia in vivo (17, 56) is well documented. Therefore, the fast ATP-independent response of the proton pump to glucose availability in renal epithelium should be physiologically very important. In contrast, pancreatic β cells respond to glucose stimulation with an almost immediate increase in ATP level (16). Yet, glucose-dependent movements of secretory vesicles and insulin secretion by islet β cells has both ATP-dependent and ATP-independent components (53).

V-ATPase translocation by vesicular trafficking between intracellular compartments is a crucial mechanism for V-ATPase recruitment in response to physiological or developmental stimuli (11, 24, 45). Chronic acidosis induced extensive translocation of V-ATPase-containing vesicles from the cytoplasm to the plasma membrane in the collecting duct intercalated cells and in the medulla (2, 24). Inducing differentiation of the murine macrophage cell line RAW 264.7 into multinuclear osteoclast-like cells resulted in the translocation of the a3-isoform-containing V-ATPase from lysosomes and late endosomes to the cell periphery, where they fused with the plasma membrane (58). However, the molecular mechanisms involved in V-ATPase targeting to particular membrane compartments, including the apical membrane, remain largely unknown.

The results of this study confirm and extend previous observations that V-ATPases respond to regulatory factors with changes in V_1 and V_o association/dissociation. Renal epithelial cells respond to changes in glucose availability with reversible disassembly of the V-ATPase holoenzyme into V_1 and V_o domains, in a manner similar to that of yeast cells (30). In contrast to yeast cells, in LLC-PK_1 cells this effect of glucose requires active PI3K. An expression of the constitutively active

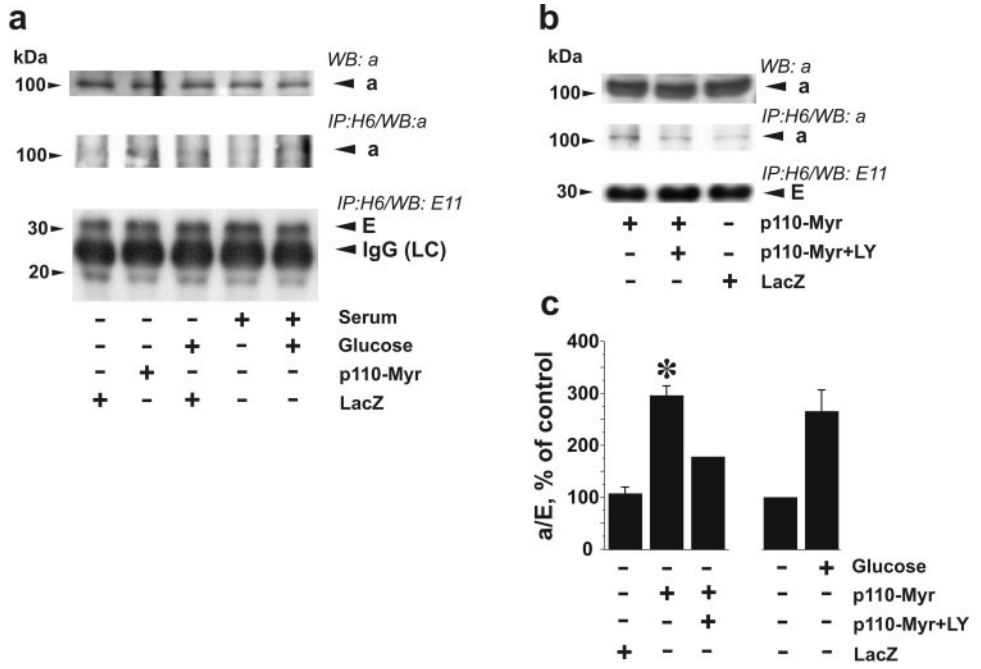

FIG. 9. Constitutively active PI3K stimulates assembly of V-ATPase in LLC-PK_1 cells in the absence of glucose. LLC-PK1 cells were cultured in standard conditions and then were infected with Adeno/Myr-p110-Myc or Adeno/LacZ at an MOI of 10 for 48 h. Then cells were transferred to glucose- and serum-free medium for 16 to 18 h followed by stimulation with 25 mM glucose for 15 min (a) or treatment with 25 μM LY294002 (LY) for 60 min (b). After stimulation, V-ATPase was immunoprecipitated from the cell lysates with H6.1 MAb. Coprecipitation of V_o and V_1 domains of V-ATPase was probed by Western blotting using antibodies against subunits a (V_o domain) and E (antibody E11, V_1 domain). The upper panels in panels a and b show immunoblot detection of the a subunit in the cell lysates before V-ATPase immunoprecipitation. (c) Densitometric analysis of the ratio of the amount of coprecipitated a and E subunits represents changes in assembly of V_1 and V_o domains. Data are presented as percentages of the control (glucose-deprived noninfected cells) as means ± standard errors of the means ($n = 2$ or 3); *, $P < 0.01$ (t test) versus LacZ-infected group.

catalytic subunit p110α of PI3K can stimulate V-ATPase assembly in the absence of glucose.

The current study demonstrates only an involvement of PI3K-dependent signaling in the control of V-ATPase trafficking, assembly, and function by glucose, whereas mechanisms upstream and downstream of PI3K remain unknown. The upstream signaling mechanism linking glucose with PI3K is poorly understood at the present time. In pancreatic β cells glucose-induced activation of PI3K involves recruitment of the adaptor proteins mSOS, IRS-2, and Grb2 to PI3K regulatory subunit p85 (29) in a fashion similar to that of the classical pathway of the PI3K activation via tyrosine kinase receptors. Activation of the tyrosine kinase receptor-dependent and -independent pathways leading to PI3K might de triggered by glucose-induced generation of reactive oxygen species (19, 37). On the other hand, PI3K catalytic subunit p110 contains domains responsible for the allosteric control of the enzyme, independent of regulatory subunit. Ras is among the few established allosteric regulators of p110 (60). Since glucose and glucose-6-phosphate are well-known physiologically relevant allosteric regulators for a variety of enzymes (for a review, see reference 4), the possibility that they could be allosteric regulators of PI3K cannot be ruled out. For the involvement of PI3K and downstream mechanisms, two scenarios might be considered a priori. (i) PI3K activation and synthesis of 3-phosphoinositides (3-PI) [PtdIns3P, PtdIns(3,4)P_2, PtdIns(3,5)P_2, and PtdIns(3,4,5)P_3] in specific membrane compartments followed by interaction with 3-PI-binding domains (PH, FYVE, PX, or the equivalent) of V-ATPase subunits or interacting proteins. (ii) PI3K-dependent activation of the downstream protein kinases, such as Akt and p70 S6K, followed by phosphorylation of the specific substrates. V-ATPase subunits or some phosphorylation state-dependent V-ATPase-interacting adaptor proteins are likely to be substrates for these and other downstream protein kinases.

It is not known whether V-ATPase subunits have 3-PI-binding domains. On the other hand, V-ATPase subunits B and C interact with F-actin (14, 28, 61), and interaction between subunit B and F-actin requires active PI3K (14). PI3K and downstream signaling, primarily via the small GTPase Rac, play a crucial role in the control of the actin cytoskeleton (60). We can suggest that the effect of glucose on V-ATPase trafficking can be mediated, at least in part, by PI3K-dependent changes in actin microfilaments. Akt and p70 S6K are two major protein kinases involved in signal transduction downstream to PI3K. They are directly activated by phosphatidylinositol 3-phosphate-dependent protein kinase PDK1 in response to activation of PI3K and synthesis of 3-PI (3, 60). In our experiments with renal proximal tubular cells, glucose induced rapid PI3K-dependent activation of both Akt and p70 S6K. So far, none of the V-ATPase subunits or interacting proteins involved in the control of V-ATPase have been identified as substrates of Akt, p70 S6K, or another PI3K-dependent protein kinase.

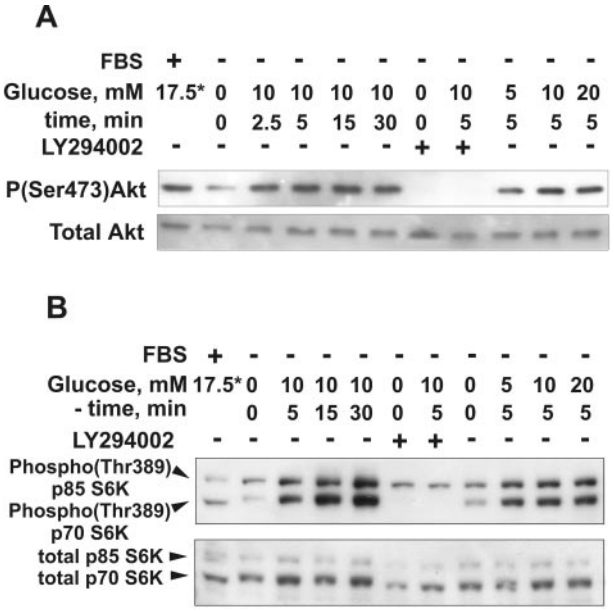

FIG. 10. Glucose induces rapid PI3K-dependent activation of Akt and p70 S6K in renal proximal tubular epithelial cells. HK-2 cells were incubated in glucose- and serum-free DMEM overnight and then were stimulated with 5 to 20 mM glucose for the indicated periods of time. If the effect of PI3K inhibition was studied, LY294002 (25 μM) and vehicle were added 30 min prior to glucose addition. The cell lysates were prepared as described in Materials and Methods, and 20-μg protein aliquots were resolved by SDS-PAGE and analyzed by immunoblotting with antibodies against phospho-Akt(Ser^{473}) and total Akt (A) or phospho-p70 S6K(Thr^{389}) and total p70 S6K (B). *, the source of glucose is serum-containing standard medium (about 5.5 and 17.5 mM for LLC-PK_1 and HK-2 cells, respectively). The results shown are representative of three independent experiments.

In summary, this study shows that glucose is a crucial regulator of V-ATPase in kidney proximal tubular cells in vitro. At physiological concentrations, glucose induces a rapid and dramatic activation of the PI3K-dependent signaling cascade. It also stimulates V-ATPase-dependent acidification of the intracellular vesicular system, assembly of V_1 and V_o domains of V-ATPase in the functional holoenzyme, and translocation V-ATPase between different cellular compartments. The presence of glucose is required for polarized distribution of V-ATPase to the apical pole of the cell. The effects of glucose require active PI3K and, in glucose-free conditions, can be reproduced by expression of the constitutively active catalytic subunit of PI3K. We propose that together with the metabolic coupling of glycolysis and V-ATPase, PI3K-dependent signaling provides a flexible multilevel mechanism for the control of V-ATPase assembly, targeting, trafficking, and proton pumping activity.

ACKNOWLEDGMENTS

This work was supported in part by NIDDK grants DK38848 and DK54362 (S.L.G.) and Gatorade research funds.

We thank W. Ogawa (Kobe University School of Medicine, Kobe, Japan) for cDNA for Myc-tagged constitutively active PI3K in pBluescript and M. Gersch for critical reading and discussion of the manuscript.

REFERENCES

1. **Anderson, R. G., J. R. Falck, J. L. Goldstein, and M. S. Brown.** 1984. Visualization of acidic organelles in intact cells by electron microscopy. Proc. Natl. Acad. Sci. USA **81:**4838–4842.
2. **Bastani, B., H. Purcell, P. Hemken, D. Trigg, and S. Gluck.** 1991. Expression and distribution of renal vacuolar proton-translocating adenosine triphosphatase in response to chronic acid and alkali loads in the rat. J. Clin. Invest. **88:**126–136.
3. **Belham, C., S. Wu, and J. Avruch.** 1999. Intracellular signalling: PDK1–a kinase at the hub of things. Curr. Biol. **9:**R93–R96.
4. **Bollen, M., S. Keppens, and W. Stalmans.** 1998. Specific features of glycogen metabolism in the liver. Biochem. J. **336**(Part 1)**:**19–31.
5. **Bowman, E. J., A. Siebers, and K. Altendorf.** 1988. Bafilomycins: a class of inhibitors of membrane ATPases from microorganisms, animal cells, and plant cells. Proc. Natl. Acad. Sci. USA **85:**7972–7976.
6. **Brandao, R. L., N. M. de Magalhaes-Rocha, R. Alijo, J. Ramos, and J. M. Thevelein.** 1994. Possible involvement of a phosphatidylinositol-type signaling pathway in glucose-induced activation of plasma membrane H(+)-ATPase and cellular proton extrusion in the yeast Saccharomyces cerevisiae. Biochim. Biophys. Acta **1223:**117–124.
7. **Brisseau, G. F., S. Grinstein, D. J. Hackam, T. Nordstrom, M. F. Manolson, A. A. Khine, and O. D. Rotstein.** 1996. Interleukin-1 increases vacuolar-type H+-ATPase activity in murine peritoneal macrophages. J. Biol. Chem. **271:** 2005–2011.
8. **Brown, D., S. Hirsch, and S. Gluck.** 1988. Localization of a proton-pumping ATPase in rat kidney. J. Clin. Invest. **82:**2114–2126.
9. **Brown, D., I. Sabolic, and S. Gluck.** 1991. Colchicine-induced redistribution of proton pumps in kidney epithelial cells. Kidney Int. Suppl. **33:**S79–S83.
10. **Brown, D., I. Sabolic, and S. Gluck.** 1992. Polarized targeting of V-ATPase in kidney epithelial cells. J. Exp. Biol. **172:**231–243.
11. **Brown, D., and J. L. Stow.** 1996. Protein trafficking and polarity in kidney epithelium: from cell biology to physiology. Physiol. Rev. **76:**245–297.
12. **Canfield, P. E., A. M. Geerdes, and B. A. Molitoris.** 1991. Effect of reversible ATP depletion on tight-junction integrity in LLC-PK1 cells. Am. J. Physiol. **261:**F1038–F1045.
13. **Cantley, L. C.** 2002. The phosphoinositide 3-kinase pathway. Science **296:** 1655–1657.
14. **Chen, S. H., M. R. Bubb, E. G. Yarmola, J. Zuo, J. Jiang, B. S. Lee, M. Lu, S. L. Gluck, I. R. Hurst, and L. S. Holliday.** 2003. Vacuolar H(super)+-ATPase binding to microfilaments: regulation in response to phosphatidylinositol 3-kinase activity and detailed characterization of the actin binding site in subunit B. J. Biol. Chem. **279:**7988–7998.
15. **Chi, M. M., M. E. Pusateri, J. G. Carter, B. J. Norris, D. B. McDougal, Jr., and O. H. Lowry.** 1987. Enzymatic assays for 2-deoxyglucose and 2-deoxyglucose 6-phosphate. Anal. Biochem. **161:**508–513.
16. **Detimary, P., G. Van den Berghe, and J. C. Henquin.** 1996. Concentration dependence and time course of the effects of glucose on adenine and guanine nucleotides in mouse pancreatic islets. J. Biol. Chem. **271:**20559–20565.
17. **Dowd, T. L., and R. K. Gupta.** 1995. NMR studies of the effect of Mg2+ on post-ischemic recovery of ATP and intracellular sodium in perfused kidney. Biochim. Biophys. Acta **1272:**133–139.
18. **Elmi, A., L. A. Idahl, and J. Sehlin.** 2000. Relationships between the Na(+)/K(+) pump and ATP and ADP content in mouse pancreatic islets: effects of meglitinide and glibenclamide. Br. J. Pharmacol. **131:**1700–1706.
19. **Esposito, F., G. Chirico, N. Montesano Gesualdi, I. Posadas, R. Ammendola, T. Russo, G. Cirino, and F. Cimino.** 2003. Protein kinase B activation by reactive oxygen species is independent of tyrosine kinase receptor phosphorylation and requires SRC activity. J. Biol. Chem. **278:**20828–20834.
20. **Forgac, M.** 1999. Structure and properties of the vacuolar (H+)-ATPases. J. Biol. Chem. **274:**12951–12954.
21. **Gluck, S., and J. Caldwell.** 1987. Immunoaffinity purification and characterization of vacuolar H+ATPase from bovine kidney. J. Biol. Chem. **262:** 15780–15789.
22. **Gluck, S., C. Cannon, and Q. Al-Awqati.** 1982. Exocytosis regulates urinary acidification in turtle bladder by rapid insertion of H^+ pumps into the luminal membrane. Proc. Natl. Acad. Sci. USA **79:**4327–4331.
23. **Gluck, S. L., B. S. Lee, S. P. Wang, D. Underhill, J. Nemoto, and L. S. Holliday.** 1998. Plasma membrane V-ATPases in proton-transporting cells of the mammalian kidney and osteoclast. Acta Physiol. Scand. Suppl. **643:**203–212.
24. **Gluck, S. L., D. M. Underhill, M. Iyori, L. S. Holliday, T. Y. Kostrominova, and B. S. Lee.** 1996. Physiology and biochemistry of the kidney vacuolar H+-ATPase. Annu. Rev. Physiol. **58:**427–445.
25. **Hanwell, D., T. Ishikawa, R. Saleki, and D. Rotin.** 2002. Trafficking and cell surface stability of the epithelial Na+ channel expressed in epithelial Madin-Darby canine kidney cells. J. Biol. Chem. **277:**9772–9779.
26. **Hayashi, M., A. Yamamoto, and Y. Moriyama.** 2002. The internal pH of synaptic-like microvesicles in rat pinealocytes in culture. J. Neurochem. **82:**698–704.
27. **Hemken, P., X. L. Guo, Z. Q. Wang, K. Zhang, and S. Gluck.** 1992. Immunologic evidence that vacuolar H+ ATPases with heterogeneous forms of

Mr = 31,000 subunit have different membrane distributions in mammalian kidney. J. Biol. Chem. **267:**9948–9957.
28. **Holliday, L. S., M. Lu, B. S. Lee, R. D. Nelson, S. Solivan, L. Zhang, and S. L. Gluck.** 2000. The amino-terminal domain of the B subunit of vacuolar H+-ATPase contains a filamentous actin binding site. J. Biol. Chem. **275:**32331–32337.
29. **Hugl, S. R., M. F. White, and C. J. Rhodes.** 1998. Insulin-like growth factor I (IGF-I)-stimulated pancreatic beta-cell growth is glucose-dependent. Synergistic activation of insulin receptor substrate-mediated signal transduction pathways by glucose and IGF-I in INS-1 cells. J. Biol. Chem. **273:**17771–17779.
30. **Kane, P. M.** 1995. Disassembly and reassembly of the yeast vacuolar H(+)-ATPase in vivo. J. Biol. Chem. **270:**17025–17032.
31. **Kane, P. M.** 2000. Regulation of V-ATPases by reversible disassembly. FEBS Lett. **469:**137–141.
32. **Kawasaki-Nishi, S., T. Nishi, and M. Forgac.** 2003. Proton translocation driven by ATP hydrolysis in V-ATPases. FEBS Lett. **545:**76–85.
33. **Kitamura, T., Y. Kitamura, S. Kuroda, Y. Hino, M. Ando, K. Kotani, H. Konishi, H. Matsuzaki, U. Kikkawa, W. Ogawa, and M. Kasuga.** 1999. Insulin-induced phosphorylation and activation of cyclic nucleotide phosphodiesterase 3B by the serine-threonine kinase Akt. Mol. Cell Biol. **19:**6286–6296.
34. **Lee, B. S., D. M. Underhill, M. K. Crane, and S. L. Gluck.** 1995. Transcriptional regulation of the vacuolar H(+)-ATPase B2 subunit gene in differentiating THP-1 cells. J. Biol. Chem. **270:**7320–7329.
35. **Lu, M., L. S. Holliday, L. Zhang, W. A. Dunn, Jr., and S. L. Gluck.** 2001. Interaction between aldolase and vacuolar H+-ATPase: evidence for direct coupling of glycolysis to the ATP-hydrolyzing proton pump. J. Biol. Chem. **276:**30407–30413.
36. **Lu, M., Y. Y. Sautin, L. S. Holliday, and S. L. Gluck.** 2003. The glycolytic enzyme aldolase mediates assembly, expression and activity of V-ATPase. J. Biol. Chem. **279:**8732–8739.
37. **Martindale, J. L., and N. J. Holbrook.** 2002. Cellular response to oxidative stress: signaling for suicide and survival. J. Cell. Physiol. **192:**1–15.
38. **Martys, J. L., C. Wjasow, D. M. Gangi, M. C. Kielian, T. E. McGraw, and J. M. Backer.** 1996. Wortmannin-sensitive trafficking pathways in Chinese hamster ovary cells. Differential effects on endocytosis and lysosomal sorting. J. Biol. Chem. **271:**10953–10962.
39. **Miura, K., S. Miyazawa, S. Furuta, J. Mitsushita, K. Kamijo, H. Ishida, T. Miki, K. Suzukawa, J. Resau, T. D. Copeland, and T. Kamata.** 2001. The Sos1-Rac1 signaling. Possible involvement of a vacuolar H(+)-ATPase E subunit. J. Biol. Chem. **276:**46276–46283.
40. **Nakamura, I., T. Sasaki, S. Tanaka, N. Takahashi, E. Jimi, T. Kurokawa, Y. Kita, S. Ihara, T. Suda, and Y. Fukui.** 1997. Phosphatidylinositol-3 kinase is involved in ruffled border formation in osteoclasts. J. Cell. Physiol. **172:**230–239.
41. **Nakamura, I., N. Takahashi, T. Sasaki, S. Tanaka, N. Udagawa, H. Murakami, K. Kimura, Y. Kabuyama, T. Kurokawa, T. Suda, et al.** 1995. Wortmannin, a specific inhibitor of phosphatidylinositol-3 kinase, blocks osteoclastic bone resorption. FEBS Lett. **361:**79–84.
42. **Nelson, N., and W. R. Harvey.** 1999. Vacuolar and plasma membrane proton-adenosinetriphosphatases. Physiol. Rev. **79:**361–385.
43. **Nishi, T., and M. Forgac.** 2002. The vacuolar (H+)-ATPases–nature's most versatile proton pumps. Nat. Rev. Mol. Cell Biol. **3:**94–103.
44. **Parra, K. J., and P. M. Kane.** 1998. Reversible association between the V1 and V0 domains of yeast vacuolar H+-ATPase is an unconventional glucose-induced effect. Mol. Cell. Biol. **18:**7064–7074.
45. **Pastor-Soler, N., V. Beaulieu, T. N. Litvin, N. Da Silva, Y. Chen, D. Brown, J. Buck, L. R. Levin, and S. Breton.** 2003. Bicarbonate regulated adenylyl cyclase (sAC) is a sensor that regulates pH-dependent V-ATPase recycling. J. Biol. Chem. **278:**49523–49529.
46. **Rodman, J. S., P. D. Stahl, and S. Gluck.** 1991. Distribution and structure of the vacuolar H^+ ATPase in endosomes and lysosomes from LLC-PK1 cells. Exp. Cell Res. **192:**445–452.
47. **Ryan, M. J., G. Johnson, J. Kirk, S. M. Fuerstenberg, R. A. Zager, and B. Torok-Storb.** 1994. HK-2: an immortalized proximal tubule epithelial cell line from normal adult human kidney. Kidney Int. **45:**48–57.
48. **Schoonderwoert, V. T., and G. J. Martens.** 2001. Proton pumping in the secretory pathway. J. Membr. Biol. **182:**159–169.
49. **Seol, J. H., A. Shevchenko, and R. J. Deshaies.** 2001. Skp1 forms multiple protein complexes, including RAVE, a regulator of V-ATPase assembly. Nat. Cell Biol. **3:**384–391.
50. **Shepherd, R. M., and J. C. Henquin.** 1995. The role of metabolism, cytoplasmic Ca2+, and pH-regulating exchangers in glucose-induced rise of cytoplasmic pH in normal mouse pancreatic islets. J. Biol. Chem. **270:**7915–7921.
51. **Smardon, A. M., M. Tarsio, and P. M. Kane.** 2002. The RAVE complex is essential for stable assembly of the yeast V-ATPase. J. Biol. Chem. **277:**13831–13839.
52. **Snowdowne, K. W., C. C. Freudenrich, and A. B. Borle.** 1985. The effects of anoxia on cytosolic free calcium, calcium fluxes, and cellular ATP levels in cultured kidney cells. J. Biol. Chem. **260:**11619–11626.
53. **Straub, S. G., and G. W. Sharp.** 2002. Glucose-stimulated signaling pathways in biphasic insulin secretion. Diabetes Metab. Res. Rev. **18:**451–463.
54. **Su, Y., A. Zhou, R. S. Al-Lamki, and F. E. Karet.** 2003. The a-subunit of the V-type H+-ATPase interacts with phosphofructokinase-1 in humans. J. Biol. Chem. **278:**20013–20018.
55. **Sumner, J. P., J. A. Dow, F. G. Earley, U. Klein, D. Jager, and H. Wieczorek.** 1995. Regulation of plasma membrane V-ATPase activity by dissociation of peripheral subunits. J. Biol. Chem. **270:**5649–5653.
56. **Taie, S., S. Yokono, M. Ueki, and K. Ogli.** 2001. Effects of ulinastatin (urinary trypsin inhibitor) on ATP, intracellular pH, and intracellular sodium transients during ischemia and reperfusion in the rat kidney in vivo. J. Anesth. **15:**33–38.
57. **Tompkins, L. S., K. D. Nullmeyer, S. M. Murphy, C. S. Weber, and R. M. Lynch.** 2002. Regulation of secretory granule pH in insulin-secreting cells. Am. J. Physiol. Cell Physiol. **283:**C429–C437.
58. **Toyomura, T., Y. Murata, A. Yamamoto, T. Oka, G. H. Sun-Wada, Y. Wada, and M. Futai.** 2003. From lysosomes to the plasma membrane: localization of vacuolar-type H+ -ATPase with the a3 isoform during osteoclast differentiation. J. Biol. Chem. **278:**22023–22030.
59. **Van Den Berg, J. G., J. Aten, C. Annink, J. H. Ravesloot, E. Weber, and J. J. Weening.** 2002. Interleukin-4 and -13 promote basolateral secretion of H(+) and cathepsin L by glomerular epithelial cells. Am. J. Physiol. Renal Physiol. **282:**F26–F33.
60. **Vanhaesebroeck, B., S. J. Leevers, K. Ahmadi, J. Timms, R. Katso, P. C. Driscoll, R. Woscholski, P. J. Parker, and M. D. Waterfield.** 2001. Synthesis and function of 3-phosphorylated inositol lipids. Annu. Rev. Biochem. **70:**535–602.
61. **Vitavska, O., H. Wieczorek, and H. Merzendorfer.** 2003. A novel role for subunit C in mediating binding of the H+-V-ATPase to the actin cytoskeleton. J. Biol. Chem. **278:**18499–18505.
62. **Wang, S. P., I. Krits, S. Bai, and B. S. Lee.** 2002. Regulation of enhanced vacuolar H+-ATPase expression in macrophages. J. Biol. Chem. **277:**8827–8834.
63. **Wieczorek, H., G. Grber, W. R. Harvey, M. Huss, H. Merzendorfer, and W. Zeiske.** 2000. Structure and regulation of insect plasma membrane H(+)V-ATPase. J. Exp. Biol. **203**(Part 1)**:**127–135.
64. **Yurko, M. A., and S. Gluck.** 1987. Production and characterization of a monoclonal antibody to vacuolar H+ATPase of renal epithelia. J. Biol. Chem. **262:**15770–15779.